

1 **Recent seismic activity at Cephalonia island (Greece): A**  
2 **study through candidate electromagnetic precursors in**  
3 **terms of nonlinear dynamics.**

4  
5 **S. M. Potirakis** <sup>1</sup>, **Y. Contoyiannis** <sup>2</sup>, **N. S. Melis** <sup>3</sup>, **J. Kopanas** <sup>4</sup>,  
6 **G. Antonopoulos** <sup>4</sup>, **G. Balasis** <sup>5</sup>, **C. Kontoes** <sup>5</sup>, **C. Nomicos** <sup>6</sup>, **K. Eftaxias** <sup>2</sup>

7  
8 [1] {Department of Electronics Engineering, Piraeus University of Applied Sciences (TEI of  
9 Piraeus), 250 Thivon and P. Ralli, Aigalao, Athens, GR-12244, Greece, [spoti@teipir.gr](mailto:spoti@teipir.gr) }.

10 [2] {Department of Physics, Section of Solid State Physics, University of Athens,  
11 Panepistimiopolis, GR-15784, Zografos, Athens, Greece, (Y. C: [yconto@yahoo.gr](mailto:yconto@yahoo.gr) ; K. E.:  
12 [ceftax@phys.uoa.gr](mailto:ceftax@phys.uoa.gr) )}

13 [3] {Institute of Geodynamics, National Observatory of Athens, Lofos Nimfon, Thissio,  
14 Athens, GR-11810, Greece, [nmelis@noa.gr](mailto:nmelis@noa.gr)}

15 [4] {Department of Environmental Technologists, Technological Education Institute (TEI) of  
16 the Ionian islands, Zakynthos, GR-29100, Greece, (J. K.: [jkopan@otenet.gr](mailto:jkopan@otenet.gr) ; G. A.:  
17 [sv8rx@teiion.gr](mailto:sv8rx@teiion.gr) )}

18 [5] {Institute for Astronomy, Astrophysics, Space Applications and Remote Sensing, National  
19 Observatory of Athens, Metaxa and Vasileos Pavlou, Penteli, Athens, GR-15236, Greece, (G.  
20 B.:[gbalasis@noa.gr](mailto:gbalasis@noa.gr) ; C. K.: [kontoes@noa.gr](mailto:kontoes@noa.gr) )}

21 [6] {Department of Electronics Engineering, Technological Education Institute (TEI) of  
22 Athens, Ag. Spyridonos, Aigaleo, Athens, GR-12210, Greece, [cconomicos@teiath.gr](mailto:cconomicos@teiath.gr)}

23

24 Correspondence to: G. Balasis ([gbalasis@noa.gr](mailto:gbalasis@noa.gr))

25

## 1 Abstract

2 The preparation process of two recent earthquakes (EQs) occurred in Cephalonia (Kefalonia)  
 3 island, Greece, [(38.22° N, 20.53° E), 26 January 2014,  $M_w = 6.0$ , depth = 21 km], and  
 4 [(38.25° N, 20.39° E), 3 February 2014,  $M_w = 5.9$ , depth = 10 km], respectively, is studied in  
 5 terms of the critical dynamics revealed in observables of the involved non-linear processes.  
 6 Specifically, we show, by means of the method of critical fluctuations (MCF), that signatures  
 7 of critical, as well as tricritical, dynamics were embedded in the fracture-induced  
 8 electromagnetic emissions (EME) recorded by two stations in locations near the epicenters of  
 9 these two EQs. It is worth noting that both, the MHz EME recorded by the telemetric stations  
 10 on the island of Cephalonia and the neighboring island of Zante (Zakynthos), reached  
 11 simultaneously critical condition a few days before the occurrence of each earthquake. The  
 12 critical characteristics embedded in the EME signals were further verified using the natural  
 13 time (NT) method. Moreover, we show, in terms of the NT method, that the foreshock  
 14 seismic activity also presented critical characteristics before each event. Importantly, the  
 15 revealed critical process seems to be focused on the area corresponding to the west  
 16 Cephalonia zone, following the seismotectonic and hazard zoning of the Ionian Islands area  
 17 near Cephalonia.

18

19 **Keywords:** Fracture-induced electromagnetic emissions; Earthquake dynamics; Criticality -  
 20 Tricriticality; Method of Critical Fluctuations; Natural Time Analysis; Seismotectonic Zone  
 21 Partitioning.

22

## 23 1. Introduction

24 The possible connection of the electromagnetic (EM) activity that is observed prior to  
 25 significant earthquakes (EQs) with the corresponding EQ preparation processes, often referred  
 26 to as seismo-electromagnetics, has been intensively investigated during the last years. Several  
 27 possible EQ precursors have been suggested in the literature (Uyeda et al., 2009a; Cicerone et  
 28 al., 2009; Hayakawa, 2013a, 2013b; Varotsos 2005; Varotsos et al., 2011b; Hayakawa et al.,  
 29 2015a, 2015b; Contoyiannis et al., 2016; Potirakis et al., 2016). The possible relation of the  
 30 field observed fracture-induced electromagnetic emissions (EME) in the frequency bands of

1 MHz and kHz, associated with shallow EQs with magnitude 6 or larger that occurred in land  
2 or near coast, has been examined in a series of publications in order to contribute to a better  
3 understanding of the underlying processes (e.g., [Eftaxias et al., 2001, 2004, 2008, 2013](#);  
4 [Kapiris et al., 2004](#); [Karamanos et al., 2006](#); [Papadimitriou et al., 2008](#); [Contoyiannis et al.,](#)  
5 [2005, 2013, 2015](#); [Eftaxias and Potirakis, 2013](#); [Potirakis et al., 2011, 2012a, 2012b, 2012c,](#)  
6 [2013, 2015](#); [Minadakis et al., 2012a, 2012b](#); [Balasis et al., 2011, 2013](#); [Donner et al., 2015](#);  
7 [Kalimeris et al., 2016](#)). Additionally, a four-stage model for the preparation of an EQ by  
8 means of its observable EM activity has been recently put forward ([Eftaxias and Potirakis,](#)  
9 [2013, and references therein](#); [Contoyiannis et al., 2015, and references therein](#)). In summary,  
10 the proposed four stages of the last part of EQ preparation process and the corresponding EM  
11 observations, for which specific features have been identified using appropriate time series  
12 analysis methods, appear in the following order ([Donner et al., 2015, and references therein](#)):  
13 1<sup>st</sup> stage: valid MHz anomaly; 2<sup>nd</sup> stage: kHz anomaly exhibiting tri-critical characteristics; 3<sup>rd</sup>  
14 stage: strong avalanche-like kHz anomaly; 4<sup>th</sup> stage: electromagnetic quiescence. It is noted  
15 that, according to the aforementioned stage model, the pre-EQ MHz EME is considered to be  
16 emitted during the fracture of a part of the Earth's crust that is characterized by high  
17 heterogeneity. During this phase the fracture is non-directional and spans over a large area  
18 that surrounds the family of large high-strength entities distributed along the fault sustaining  
19 the system. Note that for an EQ of magnitude ~6 the corresponding fracture process extends  
20 to a radius of ~120km ([Bowman et al., 1998](#)).

21 Two strong shallow EQs occurred recently in western Greece (see Fig. 1). On 26 January  
22 2014 (13:55:43 UT) an  $M_w = 6.0$  EQ, hereafter also referred to as “EQ1”, occurred on the  
23 island of Cephalonia (Kefalonia), with epicenter at (38.22° N, 20.53° E) and depth of ~16km.  
24 The second significant EQ,  $M_w = 5.9$ , hereafter also referred to as “EQ2”, occurred on the  
25 same island on 3 February 2014 (03:08:45 UT), with epicenter at (38.25° N, 20.40° E) and  
26 depth of ~11km. Various studies of the two earthquakes have already been published  
27 indicating their seismotectonic importance ([Karastathis et al., 2014](#); [Valkaniotis et al., 2014](#);  
28 [Papadopoulos et al., 2014](#); [Ganas et al., 2015](#); [Sakkas and Lagios, 2015](#); [Merryman Boncori et](#)  
29 [al., 2015](#)) as they were located on two different active faults that belong to the same seismic  
30 source zone.

1 A pair of simultaneous MHz EM signals was recorded at 41 MHz, with a sampling rate of 1  
2 sample/s, by two different stations prior to each one of the above mentioned significant  
3 shallow EQs. On 24 January 2014, two days before the  $M_w = 6.0$  Cephalonia EQ (EQ1), two  
4 telemetric stations of our EM signal monitoring network (see Fig. 1), the station of  
5 Cephalonia, located on the same island ( $38.18^\circ$  N,  $20.59^\circ$  E), and the station of Zante  
6 (Zakynthos), located on a neighboring island belonging to the same (Ionian) island complex  
7 ( $37.77^\circ$  N,  $20.74^\circ$  E), simultaneously recorded the first pair of aforementioned signals. The  
8 same picture was repeated for the second significant Cephalonia EQ,  $M_w = 5.9$  (EQ2).  
9 Specifically, both the Cephalonia and the Zante stations simultaneously recorded the second  
10 pair of aforementioned signals on 28 January 2014, six days prior to the specific EQ. Note  
11 that it has been repeatedly made clear that all the pre-EQ EME signals, which have been  
12 observed by our monitoring network, have been recorded only prior to strong shallow EQs,  
13 that have taken place on land (or near the coast-line); this fact, in combination to the recently  
14 proposed fractal geo-antenna model (Eftaxias et al., 2004; Eftaxias and Potirakis, 2013), can  
15 explain why these signals succeed to be transmitted on air. This model provides a good reason  
16 for the increased possibility of detection of such EM radiation, since a fractal geo-antenna  
17 emits significantly increased power, compared to the power that would be radiated by the  
18 same source, if a dipole antenna model was considered. It should also be noted that, none of  
19 the recordings of the other monitoring stations of our network (except from the ones of  
20 Cephalonia and Zante) presented critical characteristics before these two specific EQs.

21

22 <Figure 1 should be placed around here>

23

24 The analysis of the specific EM time series, using the method of critical fluctuations (MCF)  
25 (Contoyiannis and Diakonos, 2000; Contoyiannis et al., 2002, 2013), revealed critical  
26 features, implying that the possibly related underlying geophysical process was at critical  
27 state before the occurrence of each one of the EQs of interest. The critical characteristics  
28 embedded in the specific time series were further verified by means of the natural time (NT)  
29 method (Varotsos et al., 2011a, 2011b, Potirakis et al., 2013, 2015). The presence of the  
30 “critical point” during which any two active parts of the system are highly correlated,  
31 theoretically even at arbitrarily long distances, in other words when “everything depends on

1 everything else”, is consistent with the view that the EQ preparation process during the period  
2 that the MHz EME are emitted is a spatially extensive process. Note that this process  
3 corresponds to the first stage of the aforementioned four-stage model.

4 Moreover, we analyzed the foreshock seismic activity using the NT method; the obtained  
5 results indicate that seismicity also presented critical characteristics before each one of the  
6 two important events. This result implies that the observed EM anomaly and the associated  
7 foreshock seismic activity might be considered as “two sides of the same coin”. Last but not  
8 least, one day before the occurrence of EQ2, and five days after the corresponding critical  
9 EME signal, tricritical characteristics were revealed in the EME recorded by the Cephalonia  
10 station.

11 The remainder of this manuscript is organized as follows: A brief introduction to the MCF  
12 and the NT analysis methods is provided in Section 2. The analysis of the EME recordings  
13 according to these two methods is presented in Section 3. Section 4 presents the results  
14 obtained by the analysis of the foreshock seismic activity using the NT method, while Section  
15 5 concludes the manuscript by summarizing and discussing the findings.

16

## 17 **2. Critical Dynamics Analysis Methods**

18 Criticality has early been suggested as an EQ precursory sign (Chelidze, 1982; Chelidze and  
19 Kolesnikov, 1982; Chelidze et al., 2006; Rundle et al., 2012; Wanliss et al., 2015). Critical  
20 phenomena have been proposed as the likely framework to study the origins of EQ related  
21 EM fluctuations, suggesting that the theory of phase transitions and critical phenomena may  
22 be useful in gaining insight to the mechanism of their complex dynamics (Bowman et al.,  
23 1998; Contoyiannis et al., 2004a, 2005, 2015; Varotsos et al., 2011a, 2011b). One possible  
24 reason for the appropriateness of this model may be the way in which correlations spread  
25 thought a disordered medium/ system comprised of subunits. From a qualitative / intuitive  
26 perspective, according to the specific approach, initially single isolated activated parts emerge  
27 in the system which, then, progressively grow and proliferate, leading to cooperative effects.  
28 Local interactions evolve to long-range correlations, eventually extending along the entire  
29 system. A key point in the study of dynamical systems that develop critical phenomena is the  
30 identification of the “critical epoch” during which the “short-range” correlations evolve into  
31 “long-range” ones. Therefore, the theory of phase transitions and critical phenomena seem to

1 be appropriate for the study of dynamical complex systems in which local interactions evolve  
 2 to long-range correlations, such as the disordered Earth's crust during the preparation of an  
 3 EQ. It is worth noting that key characteristics of a critical point in a phase transition of the  
 4 second order are the existence of highly correlated fluctuations and scale invariance in the  
 5 statistical properties. By means of experiments on systems presenting this kind of criticality as  
 6 well as by appropriately designed numerical experiments, it has been confirmed that right at  
 7 the "critical point" the subunits are highly correlated even at arbitrarily large "distance". At  
 8 the critical state self-similar structures appear both in time and space. This fact is  
 9 quantitatively manifested by power law expressions describing the distributions of spatial or  
 10 temporal quantities associated with the aforementioned self-similar structures (Stanley, 1987,  
 11 1999).

12 The time series analysis methods employed in this paper for the evaluation of the MHz EME  
 13 recordings and the seismicity around the Cephalonia island in terms of critical dynamics are  
 14 briefly presented in the following. Specifically, the method of critical fluctuations (MCF) is  
 15 described in Sub-Section 2.1, while the natural time (NT) method is described in Sub-Section  
 16 2.2.

17

## 18 2.1 Method of critical fluctuations (MCF)

19 In the direction of comprehending the dynamics of a system undergoing a continuous phase  
 20 transition at critical state, the method of critical fluctuations (MCF) has been proposed for the  
 21 analysis of critical fluctuations in the systems' observables (Contoyiannis and Diakonos,  
 22 2000; Contoyiannis et al., 2002). The dynamics of various dynamical systems have been  
 23 successfully analyzed by MCF; examples include thermal (e.g., 3D Ising) (Contoyiannis et  
 24 al., 2002), geophysical (Contoyiannis and Eftaxias 2008; Contoyiannis et al., 2004a, 2010,  
 25 2015, 2016), biological (electro-cardiac signals) (Contoyiannis et al., 2004b; Contoyiannis et  
 26 al., 2013) and economic systems (Ozun et al., 2014).

27 It has been shown (Contoyiannis and Diakonos, 2000) that the dynamics of the order  
 28 parameter fluctuations  $\phi$  at the critical state for a second-order phase transition can be  
 29 theoretically formulated by the non-linear intermittent map:

30 
$$\phi_{n+1} = \phi_n + u\phi_n^z, \quad (1)$$

1 where  $\phi_n$  is the scaled order parameter value at the time interval  $n$ ;  $u$  denotes an effective  
 2 positive coupling parameter describing the non-linear self-interaction of the order parameter;  
 3  $z$  stands for a characteristic exponent associated with the isothermal exponent  $\delta$  for critical  
 4 systems at thermal equilibrium ( $z = \delta + 1$ ). The marginal fixed-point of the above map is the  
 5 zero point, as expected from critical phenomena theory.

6 However, it has been shown that in order to quantitatively study a real (or numerical)  
 7 dynamical system one has to add an unavoidable “noise” term,  $\varepsilon_n$ , to Eq. (1), which is  
 8 produced by all stochastic processes (Contoyiannis and Diakonos, 2007). Note that, from the  
 9 intermittency mathematical framework point of view, the “noise” term denotes ergodicity in  
 10 the available phase space. In this respect, the map of Eq. (1), for positive values of the order  
 11 parameter, becomes:

$$12 \quad \phi_{n+1} = \left| \phi_n + u\phi_n^z + \varepsilon_n \right|. \quad (2)$$

13 Based on the map of Eq. (2), MCF has been introduced as a method capable of identifying  
 14 whether a system is in critical state of intermittent type by analyzing time-series  
 15 corresponding to an observable of the specific system. In a few words, MCF is based on the  
 16 property of maps of intermittent-type, like the ones of Eqs. (1) and (2), that the distribution of  
 17 properly defined laminar lengths (waiting times)  $l$  follow a power-law  $P(l) \sim l^{-p_l}$  (Schuster,  
 18 1998), where the exponent  $p_l$  is  $p_l = 1 + \frac{1}{\delta}$  (Contoyiannis et al., 2002). However, the  
 19 distribution of waiting times for a real data time series which is not characterized by critical  
 20 dynamics follows an exponential decay, rather than a power-law one (Contoyiannis et al.,  
 21 2004a), due to stochastic noise and finite size effects. Therefore, the dynamics of a real time  
 22 series can be estimated by fitting the distribution of waiting times (laminar lengths) to a  
 23 function  $\rho(l)$  combining both power-law and exponential decay (Contoyiannis and Diakonos,  
 24 2007):

$$25 \quad \rho(l) \sim l^{-p_2} e^{-lp_3}. \quad (3)$$

26 The values of the two exponents  $p_2$  and  $p_3$ , which result after fitting laminar lengths  
 27 distribution in a log-log scale diagram, reveal the underlying dynamics. Exact critical state  
 28 calls for  $p_3 = 0$ ; in such a case it is  $p_2 = p_l > 1$ . As a result, in order for a real system to be

1 considered to be at critical state, *both criticality conditions*  $p_2 > 1$  *and*  $p_3 \approx 0$  *have to be*  
 2 *satisfied.*

3 Note that the choice of the function  $\rho(l)$  of Eq. (3), which combines both power-law and  
 4 exponential decay, to model the distribution of waiting times was deliberately made in order  
 5 to include both these fundamentally different behaviors, i.e., the critical dynamics  
 6 (Contoyiannis et al., 2002) and the complete absence of specific dynamics (stochastic  
 7 processes) (Contoyiannis et al., 2004b), respectively. In addition, the specific function also  
 8 models intermediate behaviors (Contoyiannis and Diakonos, 2007).

9 In applying the MCF the corresponding factors of  $\rho(l)$  appear to be competitive: any increase  
 10 of the  $p_2$  exponent value corresponds to a  $p_3$  exponent value reduction and vice versa.  
 11 However, this is expected because, for example, any increase of the value of  $p_3$  exponent  
 12 signifies the departure from critical dynamics and thus the reduction of  $p_2$  exponent value.  
 13 Still, it is interesting to apply MCF analysis to observe this competition in the case of pre-  
 14 earthquake EME time-series and explore whether the obtained exponent values are consistent  
 15 with those of MCF analyzes performed on other time-series with large statistics which are  
 16 considered as references for the application of our method. This competition can be observed  
 17 even within the critical windows as shown in Figs. 2d and 3d.

18 Moreover, a special dynamics case is the one known as “tricritical crossover dynamics”. In  
 19 statistical physics, a tricritical point is a point in the phase diagram of a system at which the  
 20 two basic kinds of phase transition, that is the first order transition and the second order  
 21 transition, meet (Huang, 1987). The co-existence of three phases, specifically, the high  
 22 symmetry phase, the low symmetry phase, and an intermediate “mixing state”, is a  
 23 characteristic property of the area around this point. A passage through this area, around the  
 24 tricritical point, from the second order phase transition to the first order phase transition  
 25 through the intermediate mixing state constitutes a tricritical crossover (Huang, 1987).

26 The specific dynamics is proved to be expressed by the map (Contoyiannis et al., 2015):

$$27 \quad m_{n+1} = \left| m_n - um_n^{-z} + \varepsilon_n \right|, \quad (4)$$

28 where  $m$  stands for the order parameter. This map differs from the critical map of Eq. (2) in  
 29 the sign of the parameter  $u$  and exponent  $z$ . Note that for reasons of unified formulation we

1 use for these parameters the same notation as in the critical map of Eq. (2). At the level of  
 2 MCF analysis this dynamics is expressed by the estimated values for the two characteristic  
 3 exponents  $p_2, p_3$  values, that satisfy *the tricriticality condition*  $p_2 < 1, p_3 \approx 0$ . These values  
 4 have been characterized in (Contoyiannis and Diakonos, 2007) as a signature of tricritical  
 5 behavior.

6 Note that MCF analysis is possible only for time-series which at least present cumulative  
 7 stationarity. Therefore, a cumulative stationarity test is always performed before applying the  
 8 MCF method; examples can be found in a number of publications (e.g., Contoyiannis et al.,  
 9 2004a, 2005, 2010; Contoyiannis and Eftaxias, 2008; Potirakis et al., 2015). More details on  
 10 the application of MCF can be found in several published articles (e.g., Contoyiannis et al.  
 11 2002, 2013, 2015), as well as in Section 3 where application on the MHz EM variations is  
 12 presented.

13

## 14 2.2 Natural time method (NT)

15 The natural time method was originally proposed for the analysis for a point process like DC  
 16 (Direct Current) or ultra-low frequency ( $\leq 1$  Hz) SES (Seismic Electric Signals) (Varotsos et  
 17 al., 2002; Varotsos, 2005), and has been shown to be optimal for enhancing the signals in the  
 18 time-frequency space (Abe et al., 2005). The transformation of a time-series of “events” from  
 19 the conventional time domain to natural time domain is performed by ignoring the time-stamp  
 20 of each event and retaining only their normalized order (index) of occurrence. Explicitly, in a  
 21 time series of  $N$  successive events, the natural time,  $\chi_k$ , of the  $k^{\text{th}}$  event is the index of  
 22 occurrence of this event normalized, by dividing by the total number of the considered events,  
 23  $\chi_k = k/N$ . On the other hand, the “energy”,  $Q_k$ , of each,  $k^{\text{th}}$ , event is preserved. We note  
 24 that the quantity  $Q_k$  represents different physical quantities for various time series: for EQ  
 25 time series it has been assigned to a seismic energy released (e.g., seismic moment) (Varotsos  
 26 et al., 2005; Uyeda et al., 2009b), and for SES signals that are of dichotomous nature it  
 27 corresponds to SES pulse duration (Varotsos, 2005), while for MHz electromagnetic emission  
 28 signals that are of non-dichotomous nature, it has been attributed to the energy of fracto-  
 29 electromagnetic emission events as defined in Potirakis et al. (2013). The transformed time  
 30 series  $(\chi_k, Q_k)$  is then studied through the normalized power spectrum

1  $\Pi(\varpi) = \left| \sum_{k=1}^N p_k \exp(j\varpi\chi_k) \right|^2$ , where  $\varpi$  is the natural angular frequency,  $\varpi = 2\pi\varphi$ , with  $\varphi$   
 2 standing for the frequency in natural time, termed “natural frequency”, and  $p_k = Q_k / \sum_{n=1}^N Q_n$   
 3 corresponds to the  $k^{th}$  event’s normalized energy. Note that, the term “natural frequency”  
 4 should not be confused with the rate at which a system oscillates when it is not driven by an  
 5 external force; it defines an analysis domain dual to the natural time domain, in the  
 6 framework of Fourier–Stieltjes transform (Varotsos et al., 2011b).

7 The study of  $\Pi(\varpi)$  at  $\varpi$  close to zero reveals the dynamic evolution of the time series under  
 8 analysis. This is because all the moments of the distribution of  $p_k$  can be estimated from  
 9  $\Pi(\varpi)$  at  $\varpi \rightarrow 0$  (Varotsos et al., 2011a). Aiming to that, by the Taylor expansion  
 10  $\Pi(\varpi) = 1 - \kappa_1 \varpi^2 + \kappa_2 \varpi^4 + \dots$ , the quantity  $\kappa_1$  is defined, where  $\kappa_1 = \sum_{k=1}^N p_k \chi_k^2 - \left( \sum_{k=1}^N p_k \chi_k \right)^2$ ,  
 11 i.e., the variance of  $\chi_k$  weighted for  $p_k$  characterizing the dispersion of the most significant  
 12 events within the “rescaled” interval  $(0,1]$ . Moreover, the entropy in natural time,  $S_{nt}$ , is  
 13 defined (Varotsos et al., 2006) as  $S_{nt} = \sum_{k=1}^N p_k \chi_k \ln \chi_k - \left( \sum_{k=1}^N p_k \chi_k \right) \ln \left( \sum_{k=1}^N p_k \chi_k \right)$  and  
 14 corresponds (Varotsos et al., 2006, 2011b) to the value at  $q=1$  of the derivative of the  
 15 fluctuation function  $F(q) = \langle \chi^q \rangle - \langle \chi \rangle^q$  with respect to  $q$  (while  $\kappa_1$  corresponds to  $F(q)$  for  
 16  $q=2$ ). It is a dynamic entropy depending on the sequential order of events (Varotsos et al.,  
 17 2006). The entropy,  $S_{nt-}$ , obtained upon considering (Varotsos et al., 2006) the time reversal  
 18  $T$ , i.e.,  $Tp_m = p_{N-m+1}$ , is also considered.

19 A system is considered to approach criticality when the parameter  $\kappa_1$  converges to the value  
 20  $\kappa_1 = 0.070$  and at the same time both the entropy in natural time and the entropy under time  
 21 reversal satisfy the condition  $S_{nt}, S_{nt-} < S_u = (\ln 2/2) - 1/4$  (Sarlis et al., 2011), where  $S_u$   
 22 stands for the entropy of a “uniform” distribution in natural time (Varotsos et al., 2006).

23 In the special case of natural time analysis of foreshock seismicity (Varotsos et al., 2001,  
 24 2005, 2006; Sarlis et al., 2008), the seismicity is considered to be in a true critical state, a “true  
 25 coincidence” is achieved, when three additional conditions are satisfied: (i) The “average”

1 distance  $\langle D \rangle$  between the curves of normalized power spectra  $\Pi(\varpi)$  of the evolving  
 2 seismicity and the theoretical estimation of  $\Pi(\varpi)$ ,  
 3  $\Pi_{critical}(\varpi) = (18/5\varpi^2) - (6\cos\varpi/5\varpi^2) - (12\sin\varpi/5\varpi^3)$ ,  $\Pi_{critical}(\varpi) \approx 1 - \kappa_1\varpi^2$ , for  
 4  $\kappa_1 = 0.070$  should be smaller than  $10^{-2}$ , i.e.,  $\langle D \rangle = \langle |\Pi(\varpi) - \Pi_{critical}(\varpi)| \rangle < 10^{-2}$ ; (ii) the  
 5 parameter  $\kappa_1$  should approach the value  $\kappa_1 = 0.070$  “by descending from above” (Varotsos et  
 6 al., 2001); (iii) Since the underlying process is expected to be self-similar, the time of the true  
 7 coincidence should not vary upon changing (within reasonable limits) either the magnitude  
 8 threshold,  $M_{thres}$ , or the area, used in the calculation.

9 It should be finally clarified that in the case of seismicity analysis, the temporal evolution of  
 10 the parameters  $\kappa_1$ ,  $S_{nt}$ ,  $S_{nt-}$ , and  $\langle D \rangle$  is studied as new events that exceed the magnitude  
 11 threshold  $M_{thres}$  are progressively included in the analysis. Specifically, as soon as one more  
 12 event is included, first the time series  $(\chi_k, Q_k)$  is rescaled in the natural time domain, since  
 13 each time the  $k^{th}$  event corresponds to a natural time  $\chi_k = k/N$ , where  $N$  is the  
 14 progressively increasing (by each new event inclusion) total number of the considered  
 15 successive events; then all the parameters involved in the natural time analysis are calculated  
 16 for this new time series; this process continues until the time of occurrence of the main event.

17 More details on the application of NT on MHz EME as well as on foreshock seismicity can be  
 18 found in Potirakis et al. (2013, 2015), as well as in Sections 3 and 4, where its application on  
 19 the MHz EM variations and foreshock seismicity is presented, respectively.

20 Note that in the case of NT analysis of foreshock seismicity, the introduction of magnitude  
 21 threshold,  $M_{thres}$ , excludes some of the weaker EQ events (with magnitude below this  
 22 threshold) from the NT analysis. On the one hand, this is necessary in order to exclude events  
 23 for which the recorded magnitude is not considered reliable; depending on the installed  
 24 seismographic network characteristics, a specific magnitude threshold is usually defined to  
 25 assure data completeness. On the other hand, the use of various magnitude thresholds,  $M_{thres}$ ,  
 26 offers a means of more accurate determination of the time when criticality is reached. In some  
 27 cases, it happens that more than one time-points may satisfy the rest of NT critical state  
 28 conditions, however the time of the true coincidence is finally selected by the last condition

1 that “true coincidence should not vary upon changing (within reasonable limits) either the  
 2 magnitude threshold,  $M_{thres}$ , or the area, used in the calculation.”

3 **3. Electromagnetic Emissions Analysis Results**

4 Part of the MHz recordings of the Cephalonia station associated with the  $M_w = 6.0$  EQ (EQ1)  
 5 is shown in Fig. 2a. This was recorded in day of year 24, that is  $\sim 2$  days before the occurrence  
 6 of EQ1. This stationary time series excerpt, having a total length of 2.8 h (10,000 samples)  
 7 starting at 24 Jan. 2014 (12:46:40 UT), was analyzed by the MCF method and was identified  
 8 to be a “critical window” (CW). CWs are time intervals of the MHz EME signals presenting  
 9 features analogous to the critical point of a second order phase transition (Contoyiannis et al.,  
 10 2005).

11 The main steps of the MCF analysis (e.g., Contoyiannis et al., 2013, 2015) on the specific  
 12 time series are shown in Fig. 2b- Fig. 2d. First, a distribution of the amplitude values of the  
 13 analyzed signal was obtained from which, using the method of turning points (Pingel et al.,  
 14 1999), a fixed-point, that is the start of laminar regions,  $\phi_o$  of about 700 mV was determined.  
 15 Fig. 2c portrays the obtained distribution of laminar lengths for the end point  $\phi_l = 655\text{mV}$ ,  
 16 that is the distribution of waiting times, referred to as laminar lengths  $l$ , between the fixed-  
 17 point  $\phi_o$  and the end point  $\phi_l$ , as well as the fitted function  $f(l) \propto l^{-p_2} e^{-p_3 l}$  with the  
 18 corresponding exponents  $p_2 = 1.35$ ,  $p_3 = 0.000$  with  $R^2 = 0.999$ . Note that the distribution  
 19 of laminar lengths is directly fitted to the specific model using the Levenberg-Marquardt  
 20 algorithm, while the fitting criterion is the chi-square minimization. The fitting is not done in  
 21 log-log space; the axes of Fig. 2c are logarithmic for the easier depiction of the distribution of  
 22 laminar lengths. Finally, Fig. 2d shows the obtained plot of the  $p_2$ ,  $p_3$  exponents vs.  $\phi_l$ . From  
 23 Fig. 2d it is apparent that the criticality conditions,  $p_2 > 1$  and  $p_3 \approx 0$ , are satisfied for a wide  
 24 range of end points  $\phi_l$ , revealing the power-law decay feature of the time series that proves  
 25 that the system is characterized by intermittent dynamics; in other words, the MHz time series  
 26 excerpt of Fig. 2a is indeed a CW.

27

28 <Figure 2 should be placed around here>

1  
2 Part of the MHz recordings of the Zante station associated with EQ1 is shown in Fig. 3a. This  
3 was also recorded in day of year 24, that is ~2 days before the occurrence of Cephalonia EQ1.  
4 This stationary time series excerpt, having a total length of 2.8 h (10,000 samples) starting at  
5 24 Jan. 2014 (12:46:40 UT), was also analyzed by the MCF method and was identified to be a  
6 “critical window” (CW).

7 The application of the MCF analysis on the specific time series (cf. Fig. 3), revealed that the  
8 criticality conditions,  $p_2 > 1$  and  $p_3 \approx 0$ , are satisfied for a wide range of end points  $\phi_l$ , for  
9 this signal too. In other words, this signal has also embedded the power-law decay feature that  
10 indicates intermittent dynamics, rendering it a CW..

11 <Figure 3 should be placed around here>

12  
13 After the  $M_w = 6.0$  (EQ1), ~ a week later, the second,  $M_w = 5.9$  (EQ2), occurred on the same  
14 island with a focal area a few km away from the first one. Six days earlier, both the  
15 Cephalonia and Zante stations simultaneously recorded MHz EME. Specifically, a stationary  
16 time series excerpt, having a total length of 3.3 h (12,000 samples) starting at 28 Jan. 2014  
17 (05:33:20 UT), from Cephalonia station and a stationary time series excerpt, having a total  
18 length of 5 h (18,000 samples) starting at 28 Jan. 2014 (03:53:20 UT), from Zante station  
19 were analyzed by the MCF method and both of them were identified to be CWs. Note that the  
20 Cephalonia CW was emitted within the time frame in which the Zante CW was emitted. Figs  
21 4 & 5 show the results of the corresponding analyses.

22  
23 <Figure 4 should be placed around here>

24  
25 <Figure 5 should be placed around here>

26  
27 In summary, we conclude that, according to the MCF analysis method, both stations recorded  
28 MHz signals that simultaneously presented critical state features two days before the first  
29 main event and six days before the second main event. In order to verify this finding, we

1 proceeded to the analysis of all the corresponding MHz signals by means of the NT analysis  
2 method, according to the way of application proposed in [Potirakis et al. \(2013\)](#). According to  
3 the specific procedure for the application of the NT method on the MHz signals, we  
4 performed an exhaustive search seeking for at least one amplitude threshold value (applied  
5 over the total length of the analyzed signal), for which the corresponding fracto-EME events  
6 satisfy the natural time method criticality conditions. The idea is that if the MCF gives valid  
7 information, and as a consequence the analyzed time series excerpt is indeed in critical  
8 condition, then there should be at least one threshold value for which the NT criticality  
9 conditions (cf. Sec. 2.2) are satisfied. Indeed, as apparent from Fig. 6, all four signals satisfy  
10 the criticality conditions according to the NT method for at least one of the considered  
11 threshold values, therefore the results obtained by the MCF method are successfully verified.

12

13 &lt;Figure 6 should be placed around here&gt;

14

15 On 2 February 2014, i.e., one day before the occurrence of EQ2, MHz EME presenting  
16 tricritical characteristics was recorded by the Cephalonia station. This signal emerged five  
17 days after the CWs that were identified in the simultaneously recorded, by the Cephalonia and  
18 Zante stations, MHz EME. The specific MHz time series excerpt from Cephalonia station,  
19 having a total length of 7.5 h (27,000 samples) starting at 2 Feb. 2014 (07:46:40 UT), was  
20 analyzed by means of the MCF method yielding the results shown in Fig. 7. As apparent from  
21 the results, this signal satisfies the tricriticality conditions  $p_2 < 1$ ,  $p_3 \approx 0$  (cf. Sec. 2.1) for a  
22 wide range of end points  $\phi$ , revealing the intermediate “mixing state” between the second  
23 order phase transition to the first order phase transition. Unfortunately, during the time that  
24 the Cephalonia station recorded tricritical MHz signal, the Zante station was not in operation;  
25 actually, it was out of operation for several hours during the specific day.

26

27 &lt;Figure 7 should be placed around here&gt;

28

1 It has been recently found (Contoyiannis et al., 2015) that such a behavior is identified in the  
2 kHz EME which usually emerge near the end of the MHz EME when the environment in  
3 which the EQ preparation process evolves changes from heterogeneous to less heterogeneous,  
4 and before the emergence of the strong avalanche-like kHz EME which have been attributed  
5 to the fracture of the asperities sustaining the fault. Actually, this has been proposed as the  
6 second stage of the four-stage model for the preparation of an EQ by means of its observable  
7 EM activity (Eftaxias and Potirakis, 2013, and references therein; Contoyiannis et al., 2015,  
8 and references therein; Donner et al., 2015). The identification of tricritical behavior in MHz  
9 EME is a quite important finding, indicating that the tricritical behavior, attributed to the  
10 second stage of the aforementioned four-stage model, can be identified either in kHz or in  
11 MHz EME, leading thus to a revision of the specific four-stage model in order to include this  
12 case too.

13 As a conclusion, after the first stage of the EQ preparation process where MHz EME with  
14 critical features are emitted, a second stage follows where MHz or kHz or both MHz and kHz  
15 EME with tricritical features are emitted. As already mentioned (cf. Sec. 2.1), in terms of  
16 statistical physics the tricritical behavior is an intermediate dynamical state which is  
17 developed in the region of the phase diagram of a system around the tricritical point, which  
18 can be approached either from the edge of the first order phase transition (characterizing the  
19 strong avalanche-like kHz EME attributed to the third stage of the four-stage model) or from  
20 the edge of the second order phase transition (characterizing the critical MHz EME attributed  
21 to the first stage of the four-stage model). Therefore, although it is expected that the tricritical  
22 behavior will be rarely observed, as it has already been discussed in (Contoyiannis et al.,  
23 2015), it can be found either in MHz time series, following the emission of a critical MHz  
24 EME, or in kHz time series preceding the emission of avalanche-like kHz EME.

25

#### 26 **4. Foreshock Seismic Activity Analysis Results**

27 As already mentioned in Potirakis et al. (2013, 2015): “seismicity and pre-fracture EMEs  
28 should be two sides of the same coin concerning the EQ generation process. If the MHz  
29 EMEs and the corresponding foreshock seismic sequence are observable manifestations of the  
30 same complex system at critical state, both should be possible to be described as a critical  
31 phenomenon by means of the natural time method.” Therefore, we also proceeded to the

1 examination of the corresponding foreshock seismic activity around Cephalonia before each  
2 one of the significant EQs of interest in order to verify this suggestion. However, we did not  
3 apply the NT method on concentric circles around the epicenter of each EQ, as in [Potirakis et](#)  
4 [al. \(2013, 2015\)](#), but instead we decided to study seismicity within areas determined  
5 according to seismotectonic and earthquake hazard criteria.

6 Following the detailed study presented in [Vamvakaris et al. \(2016\)](#), we incorporated the  
7 seismic zones proposed there for our area of study. Thus, as it is presented in Fig. 8, we  
8 defined five separate seismic zones, based on the criteria explored in [Vamvakaris et al. \(2016\)](#)  
9 and the seismic zonation proposed by them. Since the study area, comprises the most  
10 seismically active zone in Greece, assigned also the highest value on the Earthquake Building  
11 Code for the country, a large number of source, stress and strain studies have been used in  
12 their study to establish such definition of zoning. Hence, it was found well justified to follow  
13 their zone definition. In Fig. 8, from east to west and north to south, one can identify the  
14 zones of Akarnania (area no. 1), Lefkada island (area no. 2), east Cephalonia island (area no.  
15 3), west Cephalonia island (area no. 4), and Zante island (area no. 5), respectively, covering  
16 the area of the Ionian Sea near Cephalonia island.

17

18 <Figure 8 should be placed around here>

19

20 Before we proceed to the NT analysis of seismicity, the seismic activity prior to EQ1, as well  
21 as between EQ1 and EQ2 is briefly discussed in relation to the above mentioned seismic  
22 zones. Earthquake parametric data have been retrieved from the National Observatory of  
23 Athens on-line catalogue (<http://www.gein.noa.gr/en/seismicity/earthquake-catalogs>), while  
24 for all the presented maps and calculations the local magnitude ( $M_L$ ), as provided by the  
25 specific earthquake catalog, is used. The foreshock seismic activity before EQ1 for the whole  
26 investigated area of the Ionian Sea region from 13 December 2013 up to the time of  
27 occurrence of the main event is shown in the map of Fig. 9a. As it can be easily observed  
28 from this map, there was a high seismic activity mainly focused on two specific zones: west  
29 Cephalonia and Zante. Notably, an EQ of  $M_L = 4.7$  occurred in Zante on 11/01/2014  
30 04:12:58, indicated by the black arrow in Fig. 9a. No EQs were recorded in Akarnania, while

1 very few events were recorded in Lefkada and east Cephalonia. The events which occurred in  
 2 west Cephalonia are also shown in a separate map in Fig. 9b for later reference.

3

4 <Figure 9 should be placed around here>

5

6 Applying the natural time analysis on seismic data (cf. Sec. 2.2), the evolution of the time  
 7 series ( $\chi_k, Q_k$ ) was studied for the foreshock seismicity prior to EQ1, where  $Q_k$  is in this  
 8 case the seismic energy released during the  $k^{th}$  event. The seismic moment,  $M_0$ , as  
 9 proportional to the seismic energy, is usually considered (Varotsos et al., 2005; Uyeda et al.,  
 10 2009b; Potirakis et al., 2013,2015). Our calculations were based on the seismic moment  $M_0$   
 11 (in dyn.cm) resulting from the corresponding  $M_L$  as (Varotsos et al., 2005; Potirakis et al.,  
 12 2013, 2015),  $M_0 = 10^{0.99M_L + 11.8}$ . First, we performed an NT analysis on the seismicity activity  
 13 of the whole investigated Ionian Sea region during the period from 13/12/2013 00:00:00 to  
 14 26/01/2014 13:55:44 UT, i.e., just after the occurrence of EQ1, for different magnitude  
 15 thresholds,  $M_{thres}$ , for which all earthquakes having  $M_L > M_{thres}$  were included in the analysis.  
 16 Note that, only  $M_{thres} \geq 2$  was considered in order to assure data completeness (Chouliaras et  
 17 al., 2013a, 2013b).

18 For all the considered threshold values, the result was the same: no indication of criticality  
 19 was identified (see for example Fig. 10a). Since, as we have already mentioned, the whole  
 20 investigated area was mainly dominated by the seismic activity in west Cephalonia and the  
 21 seismic activity in Zante, while an EQ of  $M_L = 4.7$  occurred in Zante, we decided to start the  
 22 NT analysis after the occurrence of the specific Zante EQ, in order to exclude from our  
 23 analysis possible foreshock activity related to the specific event. As a result, we performed  
 24 NT analysis for the time period 11/01/2014 04:13:00 (just after the  $M_L = 4.7$  Zante EQ) to  
 25 26/01/2014 13:55:44 UT, for different magnitude thresholds in three successively enclosed  
 26 areas: namely, the whole investigated area of Ionian Islands region, both Cephalonia (east and  
 27 west) zones combined, and the zone of west Cephalonia. Representative examples of these  
 28 analyses are depicted in Fig. 10b – Fig. 10d. The analysis over the whole investigated area of  
 29 the Ionian Islands region indicates that seismicity reaches criticality on 19 and 20 of January,

1 while the two other progressively narrower areas indicate that the criticality conditions  
2 according to NT method are satisfied on 19 and 22 of January. These results imply that  
3 seismicity was also in critical condition a few days prior to the occurrence of the first studied  
4 significant Cephalonia EQ (EQ1). Actually, in the specific case, the critical condition of  
5 seismicity was reached before, but quite close, to the emission of the corresponding MHz  
6 signals for which critical behavior was identified (cf. Sec. 3). Note that a very recent analysis  
7 on the foreshock seismic activity before EQ1, in terms of a combination of multiresolution  
8 wavelets and NT analysis, which was performed on concentric areas of 50 km and 30 km  
9 radii around the epicenter of EQ1, also found that NT analysis criticality requirements are met  
10 a few days before EQ1 (at approximately 20 January) (Vallianatos et al., 2015).

11

12 <Figure 10 should be placed around here>

13

14 Before the application of the NT method to the seismic activity prior to EQ2, one should first  
15 study the time evolution of the activity between the two significant events of interest, in order  
16 to minimize if possible the influence of the first EQ aftershock sequence on the NT analysis.  
17 Our first observation about the EQs which occurred during the specific time period was that,  
18 all but one had epicenters in west Cephalonia. Only one  $M_L = 2.3$  EQ occurred in Zante, at  
19 ( $37.79^\circ$  N,  $21.00^\circ$  E) on 28 January 2014 02:08:27 UT.

20 Fig. 11a shows all the events that were recorded in the whole investigated area of the Ionian  
21 Islands region vs. time from just after EQ1 ( $M_w = 6.0$ ) up to the time of EQ2 ( $M_w = 5.9$ ),  
22 including EQ2. As it can be seen, if one considers that both significant EQs of interest were  
23 main events, it is quite difficult to separate the seismic activity of the specific time period into  
24 aftershocks of the first EQ and foreshocks of the second one. However, we observe that up to  
25 a specific time point, there is a rapid decrease of the running mean magnitude of the recorded  
26 EQs, while after that the long range (75 events) running mean value seems to be almost  
27 constant over time with the short range (25 events) one varying around it. We arbitrarily set  
28 the 29 January 00:00:00 UT as the time point after which the recorded seismicity is no longer  
29 dominated by the aftershocks of EQ1; this by no means implies that the aftershock sequence  
30 of the EQ1 stops after that date. It should also be underlined that changing this, arbitrarily

1 selected, date within reasonable limits, does not significantly changes the results of our  
 2 corresponding NT analysis which are presented next. On the other hand, a significant shift of  
 3 this limit towards EQ1, i.e., to earlier dates, results to severe changes indicating the  
 4 domination of the recorded seismicity by the aftershock sequence of EQ1. Accordingly, the  
 5 considered as foreshock seismic activity before EQ2, i.e., from 29/01/2014 00:00 UT up to  
 6 the time of occurrence of EQ2, is presented in the map of Fig. 11b for west Cephalonia and  
 7 analyzed in the following.

8

9 <Figure 11 should be placed around here>

10

11 Next, we applied the NT method on the seismicity of west Cephalonia for the time period  
 12 from 29/01/2014 00:00:00 to 03/02/2014 03:08:47 UT. Note that we also applied the NT  
 13 method on the whole investigated area of the Ionian Islands region, obtaining practically the  
 14 same results. As we have already mentioned, only one  $M_L = 2.3$  EQ occurred outside the  
 15 west Cephalonia zone, so, on the one hand for magnitude threshold values  $M_{thres} \geq 2.3$  this  
 16 event was excluded, while, on the other hand, even for lower threshold values  
 17 ( $2 \leq M_{thres} < 2.3$ ) its inclusion does not change the results significantly. Fig. 12 shows the NT  
 18 analysis results for some threshold values proving that seismicity reaches criticality on 1 or 2  
 19 February 2014, that is one or two days before the occurrence of the second significant EQ of  
 20 interest ( $M_w = 5.9$ ). Actually, in the specific case, the critical condition of seismicity was  
 21 reached after, but quite close, to the emission of the corresponding MHz signals for which  
 22 critical behavior was identified (cf. Sec. 3).

23

24 <Figure 12 should be placed around here>

25

## 26 5. Discussion - Conclusions

27 Based on the methods of critical fluctuations and natural time, we have shown that the  
 28 fracture-induced MHz EME recorded by two stations in our network prior to two recent

1 significant EQs occurred in Cephalonia present criticality characteristics, implying that they  
2 emerge from a system in critical state.

3 There are two key points that render these observations unique in the up to now research on  
4 the pre-EQ EME:

5 (i) Although not previously reported, we have to note here that, as it has been observed, the  
6 Cephalonia station is insensitive to EQ preparation processes happening outside of the wider  
7 area of Cephalonia island, as well as to EQ preparation processes leading to low magnitude  
8 EQs within the area of Cephalonia island. Note that the only signal that has been previously  
9 recorded refers to the M=6 EQ that occurred on the specific island in 2007 ([Contoyiannis et  
al., 2010](#)).

11 (ii) Prior to each one of the studied significant EQs, two MHz EME time series presenting  
12 critical characteristics were recorded simultaneously in two different stations very close to the  
13 focal areas, while no other station of our network (cf. Fig. 1) recorded such signals prior to the  
14 specific EQs. This indicates that the revealed criticality was not associated with a global  
15 phenomenon, such as critical variations in the Ionosphere, but was rather local to the area of  
16 the Ionian Islands region, enhancing the hypothesis that these EME were associated with the  
17 EQ preparation process taking place prior to the two significant EQs. This feature, combined  
18 with the above mentioned sensitivity of the Cephalonia station only to significant EQs  
19 occurring on the specific island, could have been considered as an indication of the location of  
20 the impending EQs.

21 Electromagnetic emissions, as a phenomenon rooted in the damage process, should be an  
22 indicator of memory effects. Laboratory studies verify that: during cyclic loading, the level of  
23 EME increases significantly when the stress exceeds the maximum previously reached stress  
24 level (Kaizer effect). The existence of Kaizer effect predicts the EM silence during the  
25 aftershock period ([Eftaxias et al., 2013; Eftaxias and Potirakis, 2013, and references therein](#)).  
26 Thus, the appearance of the second EM anomaly may reveal that the corresponding  
27 preparation of fracture process has been organized in a new barrier.

28 We note that, according to the view that seismicity and pre-EQ EM emissions should be “two  
29 sides of the same coin” concerning the earthquake generation process, the corresponding  
30 foreshock seismic activity, as another manifestation of the same complex system, should be at  
31 critical state as well, before the occurrence of a main event. We have shown that this really

1 happens for both the significant EQs we studied. Importantly, the revealed critical process  
2 seems to be focused on an area corresponding to the west Cephalonia zone, one of the parts  
3 according to the seismotectonic and hazard zone partitioning of the wider area of the Ionian  
4 Islands.

5 To be more detailed, the foreshock seismicity associated with the first ( $M_w = 6.0$ ) EQ  
6 reached critical condition a few days before the occurrence of the main event. Specifically, it  
7 came to critical condition before, but quite close, to the emission of the corresponding MHz  
8 signals for which critical behavior was identified. The seismicity that was considered as  
9 foreshock of the second ( $M_w = 5.9$ ) EQ also reached criticality a few days before the  
10 occurrence of the main event. In contrary to the first EQ case, it reached criticality after, but  
11 quite close, to the emission of the corresponding MHz signals for which critical behavior was  
12 identified.

13 One more outcome of our study was the identification of tricritical crossover dynamics in the  
14 MHz emissions recorded just before the occurrence of the second significant EQ of interest  
15 ( $M_w = 5.9$ ) at the Cephalonia station. Note that, unfortunately, the Zante station was out of  
16 order for several hours during the specific day, including the time window during which the  
17 tricritical features were identified in the Cephalonia recordings. As a result, we could not  
18 cross check whether tricritical signals simultaneously also reached Zante. This is considered a  
19 quite important finding, since it verifies a theoretically expected situation, namely the  
20 approach of the intermediate dynamical state of tricritical crossover, either from the first or  
21 from the second order phase transition state. In terms of pre-EQ EME, this leads to a revision  
22 of the four-stage model for the preparation of an EQ by means of its observable EM activity.  
23 Namely, after the first stage of the EQ preparation process where MHz EME with critical  
24 features are emitted, a second stage follows where MHz or kHz or both MHz and kHz EME  
25 with tricritical features are emitted. Specifically, the tricritical crossover dynamics can be  
26 identified either in MHz time series, following the emission of a critical MHz EME, or in kHz  
27 time series preceding the emission of avalanche-like kHz EME. In summary, the proposed  
28 four stages of the last part of EQ preparation process and the associated, appropriately  
29 identified, EM observables appear in the following order: 1<sup>st</sup> stage: valid MHz anomaly; 2<sup>nd</sup>  
30 stage: MHz or kHz or MHz and kHz anomaly exhibiting tri-critical characteristics; 3<sup>rd</sup> stage:  
31 strong avalanche-like kHz anomaly; 4<sup>th</sup> stage: electromagnetic quiescence. Note that the

1 specific four-stage model is a suggestion that seems to be verified by the up to now available  
2 MHz-kHz observation data and corresponding time-series analyzes, while a rebuttal has not  
3 appeared in the literature. However, the understanding of the physical processes involved in  
4 the preparation of an EQ and their relation to various available observables is an open  
5 scientific issue. A lot of efforts still remain to be undertaken before one can claim clear  
6 understanding of EQ preparation processes and their associated possible precursors.

7 As it has been repeatedly pointed out in previous works (e.g., [Eftaxias et al., 2013](#); [Eftaxias](#)  
8 [and Potirakis, 2013, and references therein](#)), our view is that such observations and the  
9 associated analyses offer valuable information towards understanding of processes in the  
10 Earth system taking place prior to the occurrence of a significant EQ. As it is known, a large  
11 number of other precursory phenomena are also observed, both by ground and satellite  
12 stations, prior to significant EQs. Only a combined evaluation of our observations with other  
13 well documented precursory phenomena could possibly render our observations useful for a  
14 reliable short-term forecast solution. Unfortunately, in the cases of the Cephalonia EQs under  
15 study this requirement was not fulfilled. To the best of our knowledge, only one paper  
16 reporting the emergence of VLF seismic-ionospheric disturbances four days before the first  
17 Cephalonia EQ ([Skeberis et al., 2015](#)) has been published up to now. It is very important that  
18 the specific disturbances, which also correspond to a spatially extensive process as happens  
19 with the MHz EME, were recorded during the same time window with the herein presented  
20 MHz critical signals. However, more precursory phenomena could have been investigated if  
21 appropriate observation data were available. For example, if ground-based magnetic  
22 observatories in the area of Greece had available magnetometer data for the time period of  
23 interest, EQ-related ULF magnetic field variations, could also be investigated. Such ULF  
24 variations, either of lithospheric or ionospheric origin, are also a result of spatially extensive  
25 processes and have been shown to present critical characteristics prior to significant EQ  
26 occurrence ([Hayakawa et al., 2015a, 2015b](#); [Contoyiannis et al., 2016](#); [Potirakis et al., 2016](#)).

27

## 28 **Acknowledgements**

29 The authors S. M. P., Y. C., N. S. M., J. K., G. A., C. N. and K. E. would like to acknowledge  
30 that this research was co-funded by the EU (European Social Fund) and national funds, action  
31 “Archimedes III—Funding of research groups in T.E.I.”, under the Operational Programme

1 “Education and Lifelong Learning 2007-2013”. The authors G. B. and C. K. would like to  
 2 acknowledge support from the European Union Seventh Framework Programme (FP7-  
 3 REGPOT-2012-2013-1) under grant agreement no. 316210 (BEYOND – Building Capacity  
 4 for a Centre of Excellence for EO-based monitoring of Natural Disasters).

5

## 6 REFERENCES

7 Abe, S., Sarlis, N. V., Skordas, E. S., Tanaka, H. K., Varotsos, P. A.: Origin of the usefulness  
 8 of the natural-time representation of complex time series, *Phys. Rev. Lett.*, 94, doi:  
 9 10.1103/PhysRevLett.94.170601, 2005.

10 Balasis, G., Daglis, I. A., Anastasiadis, A., Papadimitriou, C., Mandea, M., Eftaxias, K.:  
 11 Universality in solar flare, magnetic storm and earthquake dynamics using Tsallis  
 12 statistical mechanics, *Physica A*, doi:10.1016/j.physa.2010.09.029, 390, 341–346, 2011.

13 Balasis, G., Donner, R. V., Potirakis, S. M., Runge, J., Papadimitriou, C., Daglis, I. A.,  
 14 Eftaxias, K., Kurths, J. : Statistical mechanics and information-theoretic perspectives on  
 15 complexity in the Earth System, *Entropy*, 15(11), 4844-4888; doi:10.3390/e15114844,  
 16 2013.

17 Bowman, D., Ouillon, G., Sammis, C., Sornette, A., Sornette, D.: An observational test of the  
 18 critical earthquake concept, *J. Geophys. Res.*, 103, 24359-24372, doi:  
 19 10.1029/98JB00792, 1998.

20 Chelidze, T.: Percolation and fracture, *Phys. Earth Planet. In.*, 28, 93-101, 1982.

21 Chelidze, T., Kolesnikov, Yu. M.: Percolation modell des bruchprozesses, *Gerlands Beitr.  
 22 Geophysik. Leipzig*, 91, 35-44, 1982.

23 Chelidze, T., Kolesnikov, Yu., Matcharashvili, T.: Seismological criticality concept and  
 24 percolation model of fracture, *Geophys. J. Int.*, 164, 125-136, 2006.

25 Chouliaras, G., Melis, N. S., Drakatos, G., Makropoulos, K.: Operational network  
 26 improvements and increased reporting in the NOA (Greece) seismicity catalog,  
 27 *Geophysical Research Abstracts*, 15, EGU2013-12634-6., 2013a.

28 Chouliaras, G., Melis, N. S., Drakatos, G., Makropoulos, K.: Operational network  
 29 improvements and increased reporting in the NOA (Greece) seismicity catalog, *Adv.  
 30 Geosci.*, 36, 7-9, doi: 10.5194/adgeo-36-7-2013, 2013b.

31 Cicerone, R. D., Ebel, J. E., Britton, J.: A systematic compilation of earthquake precursors,  
 32 *Tectonophysics*, 476, 371-396, doi: 10.1016/j.tecto.2009.06.008, 2009.

33 Contoyiannis, Y., Diakonos, F.: Criticality and intermittency in the order parameter space,  
 34 *Phys. Lett. A*, 268, 286 -292, doi: 10.1016/S0375-9601(00)00180-8, 2000.

35 Contoyiannis, Y., Diakonos, F., Malakis, A.: Intermittent dynamics of critical fluctuations,  
 36 *Phys. Rev. Lett.*, 89, 035701, doi: 10.1103/PhysRevLett.89.035701, 2002.

1 Contoyiannis, Y. F., Diakonos, F. K., Kapiris, P. G., Peratzakis, A. S., Eftaxias, K. A.:  
2 Intermittent dynamics of critical pre-seismic electromagnetic fluctuations, *Phys.*  
3 *Chem. Earth*, 29, 397-408, doi: 10.1016/j.pce.2003.11.012, 2004a.

4 Contoyiannis, Y. F., Diakonos, F. K., Papaefthimiou, C., Theophilidis, G.: Criticality in the  
5 relaxation phase of a spontaneously contracting atria isolated from a Frog's Heart,  
6 *Phys. Rev. Lett.*, 93, 098101, doi: 10.1103/PhysRevLett.93.098101, 2004b.

7 Contoyiannis, Y. F., Kapiris, P. G., Eftaxias, K. A.: A Monitoring of a pre-seismic phase from  
8 its electromagnetic precursors, *Phys. Rev. E*, 71, 066123, 066123/1-14, doi:  
9 10.1103/PhysRevE.71.066123, 2005.

10 Contoyiannis, Y. F., Diakonos, F. K.: Unimodal maps and order parameter fluctuations in the  
11 critical region, *Phys. Rev. E*, 76, 031138, 2007.

12 Contoyiannis, Y. F., Eftaxias, K.: Tsallis and Levy statistics in the preparation of an  
13 earthquake, *Nonlin. Processes Geophys.*, 15, 379-388, doi:10.5194/npg-15-379-  
14 2008, 2008.

15 Contoyiannis, Y. F., Nomicos, C., Kopanas, J., Antonopoulos, G., Contoyianni, L., Eftaxias,  
16 K.: Critical features in electromagnetic anomalies detected prior to the L'Aquila  
17 earthquake, *Physica A*, 389, 499-508, doi: 10.1016/j.physa.2009.09.046, 2010.

18 Contoyiannis, Y. F., Potirakis, S. M., Eftaxias, K.: The Earth as a living planet: human-type  
19 diseases in the earthquake preparation process, *Nat. Hazards Earth Syst. Sci.*, 13,  
20 125-139, doi: 10.5194/nhess-13-125-2013, 2013.

21 Contoyiannis, Y., Potirakis, S. M., Eftaxias, K., Contoyianni, L.: Tricritical crossover in  
22 earthquake preparation by analyzing preseismic electromagnetic emissions, *J.*  
23 *Geodynamics*, 84, 40-54, doi: 10.1016/j.jog.2014.09.015, 2015.

24 Contoyiannis, Y., Potirakis, S. M., Eftaxias, K., Hayakawa, M., Schekotov, A.: Intermittent  
25 criticality revealed in ULF magnetic fields prior to the 11 March 2011 Tohoku  
26 earthquake (Mw=9), *Physica A*, 452, 19-28, doi:10.1016/j.physa.2016.01.065, 2016.

27 Donner, R. V., Potirakis, S. M., Balasis, G., Eftaxias, K., Kurths, J.: Temporal correlation  
28 patterns in pre-seismic electromagnetic emissions reveal distinct complexity profiles  
29 prior to major earthquakes, *Phys. Chem. Earth*, 85-86, 44-55,, doi:  
30 10.1016/j.pce.2015.03.008, 2015.

31 Eftaxias, K., Kapiris, P., Polygiannakis, J., Bogris, N., Kopanas, J., Antonopoulos, G.,  
32 Peratzakis, A., Hadjicontis, V.: Signatures of pending earthquake from electromagnetic  
33 anomalies, *Geophys. Res. Lett.*, 28, 3321-3324, doi: 10.1029/2001GL013124, 2001.

34 Eftaxias, K., Frangos, P., Kapiris, P., Polygiannakis, J., Kopanas, J., Peratzakis, A.,  
35 Skountzos, P., Jaggard, D.: Review and a model of pre-seismic electromagnetic  
36 emissions in terms of fractal electrodynamics, *Fractals*, 12, 243-273, doi:  
37 10.1142/S0218348X04002501, 2004.

1 Eftaxias, K., Contoyiannis, Y., Balasis, G., Karamanos, K., Kopanas, J., Antonopoulos, G.,  
2 Koulouras, G., Nomicos, C.: Evidence of fractional-Brownian-motion-type asperity  
3 model for earthquake generation in candidate pre-seismic electromagnetic emissions,  
4 Nat. Hazards Earth Syst. Sci., 8, 657–669, doi:10.5194/nhess-8-657-2008, 2008.

5 Eftaxias, K., Potirakis, S. M., Chelidze, T.: On the puzzling feature of the silence of  
6 precursory electromagnetic emissions, Nat. Hazards Earth Syst. Sci., 13, 2381-2397,  
7 doi: 10.5194/nhess-13-2381-2013, 2013.

8 Eftaxias, K., Potirakis, S. M.: Current challenges for pre-earthquake electromagnetic  
9 emissions: shedding light from micro-scale plastic flow, granular packings, phase  
10 transitions and self-affinity notion of fracture process, Nonlin. Processes Geophys., 20,  
11 771–792, doi:10.5194/npg-20-771-2013, 2013.

12 Ganas, A., Cannavo, F., Chousianitis, K., Kassaras, I., Drakatos, G.: Displacements recorded  
13 on continuous GPS stations following the 2014 M6 Cephalonia (Greece) earthquakes:  
14 Dynamic characteristics and kinematic implications, Acta Geodyn. Geomater., 12(1), 5–  
15 27, doi: 10.13168/AGG.2015.0005, 2015.

16 Hayakawa, M. (ed.): *The Frontier of Earthquake Prediction Studies*, Nihon-Senmontoshō-  
17 Shuppan, Tokyo, 2013a.

18 Hayakawa, M. (ed.): *Earthquake Prediction Studies: Seismo Electromagnetics*, Terrapub,  
19 Tokyo, 2013b.

20 Hayakawa, M., Schekotov, A, Potirakis, S., Eftaxias, K.: Criticality features in ULF magnetic  
21 fields prior to the 2011 Tohoku earthquake, Proc. Japan Acad., Ser. B, 91, 25-30,  
22 doi: 10.2183/pjab.91.25, 2015a.

23 Hayakawa, M., Schekotov, A, Potirakis, S. M., Eftaxias, K., Li, Q., Asano, T., An Integrated  
24 Study of ULF Magnetic Field Variations in Association with the 2008 Sichuan  
25 Earthquake, on the Basis of Statistical and Critical Analyses”, Open J. Earthq. Res.,  
26 4, 85-93, doi: 10.4236/ojer.2015.43008, 2015b.

27 Huang, K.: *Statistical Mechanics*, 2<sup>nd</sup> Ed. John Wiley and sons, New York, 1987.

28 Kapiris, P., Eftaxias, K., Chelidze, T.: Electromagnetic signature of prefracture criticality in  
29 heterogeneous media, Phys. Rev. Lett., 92(6), 065702/1-4, doi:  
30 10.1103/PhysRevLett.92.065702, 2004.

31 Kalimeris, A., Potirakis, S. M., Eftaxias, K., Antonopoulos, G., Kopanas, J., Nomikos, C.:  
32 Multi-spectral detection of statistically significant components in pre-seismic  
33 electromagnetic emissions related with Athens 1999, M = 5.9 earthquake, J. App.  
34 Geophys., 128, 41–57, doi:10.1016/j.jappgeo.2016.03.002, 2016.

35 Karamanos, K., Dakopoulos, D., Aloupis, K., Peratzakis, A., Athanasopoulou, L.,  
36 Nikolopoulos, S., Kapiris, P., Eftaxias, K.: Study of pre-seismic electromagnetic signals  
37 in terms of complexity, Phys. Rev. E, 74, 016104/1-21, doi:  
38 10.1103/PhysRevE.74.016104, 2006.

39 Karastathis, V. K., Mouzakiotis, E., Ganas, A., Papadopoulos, G. A.: High-precision  
40 relocation of seismic sequences above a dipping Moho: The case of the January-  
41 February 2014 seismic sequence in Cephalonia Isl. (Greece), Solid Earth Discuss., 6,  
42 2699-2733, doi: 10.5194/sed-6-2699-2014, 2014.

1 Merryman Boncori, J. P., Papoutsis , I., Pezzo, G., Tolomei , C., Atzori, S., Ganas, A.,  
2 Karastathis, V., Salvi, S., Kontoes, C., Antonioli, A.: The February 2014 Cephalonia  
3 earthquake (Greece): 3D deformation field and source modeling from multiple SAR  
4 techniques, *Seismol. Res. Lett.* 86(1), 1-14, doi: 10.1785/0220140126, 2015.

5 Minadakis, G., Potirakis, S. M., Nomicos, C., Eftaxias, K.: Linking electromagnetic  
6 precursors with earthquake dynamics: an approach based on nonextensive fragment and  
7 self-affine asperity models, *Physica A*, 391, 2232-2244, doi:  
8 10.1016/j.physa.2011.11.049, 2012a.

9 Minadakis, G., Potirakis, S. M., Stonham, J., Nomicos, C., Eftaxias, K.: The role of  
10 propagating stress waves in geophysical scale: Evidence in terms of nonextensivity,  
11 *Physica A*, 391(22), 5648-5657, doi:10.1016/j.physa.2012.04.030, 2012b.

12 Ozun, A., Contoyiannis, Y. F., Diakonos, F. K., Hanias, M., Magafas, L.: Intermittency in  
13 stock market dynamic, *J. Trading* 9(3), 26-33, 2014.

14 Papadimitriou, K., Kalimeri, M., Eftaxias, K.: Nonextensivity and universality in the  
15 earthquake preparation process, *Phys. Rev. E*, 77, 036101/1-14, doi:  
16 10.1103/PhysRevE.77.036101, 2008.

17 Papadopoulos, G. A., Karastathis, V. K., Koukouvelas, I., Sachpazi, M., Baskoutas, I.,  
18 Chouliaras, G., Agalos, A., Daskalaki, E., Minadakis, G., Moshou, A., Mouzakiotis, A.,  
19 Orfanogiannaki, K., Papageorgiou, A., Spanos, D., Triantafyllou, I.: The Cephalonia,  
20 Ionian Sea (Greece), sequence of strong earthquakes of January-February 2014: a first  
21 report, *Res. Geoph.*, 4:5441, 19-30, doi:10.4081/rg.2014.5441, 2014.

22 Pingel, D., Schmelcher, P., Diakonos, F. K.: Theory and examples of the inverse Frobenius-  
23 Perron problem for complete chaotic maps, *Chaos*, 9, 357-366, doi: 10.1063/1.166413,  
24 1999.

25 Potirakis, S. M., Minadakis, G., Nomicos, C., Eftaxias, K.: A multidisciplinary analysis for  
26 traces of the last state of earthquake generation in preseismic electromagnetic  
27 emissions, *Nat. Hazards and Earth Syst. Sci.*, 11, 2859-2879, doi:10.5194/nhess-11-  
28 2859-2011, 2011.

29 Potirakis, S. M., Minadakis, G., Eftaxias, K.: Analysis of electromagnetic pre-seismic  
30 emissions using Fisher information and Tsallis entropy, *Physica A*, 391, 300-306,  
31 doi:10.1016/j.physa.2011.08.003, 2012a.

32 Potirakis, S. M., Minadakis, G., Eftaxias, K.: Sudden drop of fractal dimension of  
33 electromagnetic emissions recorded prior to significant earthquake, *Nat. Hazards*, 64,  
34 641-650, doi:10.1007/s11069-012-0262-x, 2012b.

35 Potirakis, S. M., Minadakis, G., Eftaxias, K.: Relation between seismicity and pre-earthquake  
36 electromagnetic emissions in terms of energy, information and entropy content, *Nat.*  
37 *Hazards Earth Syst. Sci.*, 12, 1179-1183, doi:10.5194/nhess-12-1179-2012, 2012c.

38 Potirakis, S.M., Karadimitrakis, A. and Eftaxias, K.: Natural time analysis of critical  
39 phenomena: the case of pre-fracture electromagnetic emissions, *Chaos*, 23, 2, 023117.  
40 doi:10.1063/1.4807908, 2013.

41 Potirakis, S. M., Contoyiannis, Y., Eftaxias, K., Koulouras, G., and Nomicos, C.: Recent field  
42 observations indicating an earth system in critical condition before the occurrence of a

1 significant earthquake, IEEE Geosc. Remote Sens. Lett., 12(3), 631-635, doi:  
2 10.1109/LGRS.2014.2354374, 2015.

3 Potirakis, S. M., Eftaxias, K., Schekotov, A., Yamaguchi, H., Hayakawa, M.: Criticality  
4 features in ULF magnetic fields prior to the 2013 M6.3 Kobe earthquake, Ann.  
5 Geophys., 2016 (in press).

6 Rundle, J. B., Holliday, J. R., Graves, W. R., Turcotte, D. L., Tiampo, K. F., Klein, W.:  
7 Probabilities for large events in driven threshold systems, Phys. Rev. E, 86, 021106,  
8 2012.

9 Sakkas, V., Lagios, E.: Fault modelling of the early-2014 ~ M6 Earthquakes in Cephalonia  
10 Island (W. Greece) based on GPS measurements, Tectonophysics, 644-645, 184-196,  
11 doi: 10.1016/j.tecto.2015.01.010, 2015.

12 Sarlis, N. V., Skordas, E. S., Varotsos, P. A.: Similarity of fluctuations in systems exhibiting  
13 self-organized criticality, Europhys. Lett., 96, 2, doi:10.1209/0295-5075/96/28006,  
14 2011.

15 Sarlis, N. V., Skordas, E. S., Lazaridou, M. S., Varotsos, P. A.: Investigation of seismicity  
16 after the initiation of a Seismic Electric Signal activity until the main shock, Proc. Japan  
17 Acad., Ser. B., 84, 331-343, 2008.

18 Schuster, H.: *Deterministic Chaos*, VCH, Weinheim, 1998.

19 Skeberis, C., Zaharis, Z.D., Xenos, T.D., Spatalas, S., Arabelos, D.N., Contadakis, M.E.:  
20 Time-frequency analysis of VLF for seismic-ionospheric precursor detection:  
21 Evaluation of Zhao-Atlas-Marks and Hilbert-Huang Transforms, Phys. Chem. Earth,  
22 85-86, 174–184, doi:10.1016/j.pce.2015.02.006, 2015.

23 Stanley, H. E.: *Introduction to Phase Transitions and Critical Phenomena*, Oxford University  
24 Press, New York, 1987.

25 Stanley, H. E.: Scaling, universality, and renormalization: Three pillars of modern critical  
26 phenomena, Rev. Modern Phys., 71, S358-S366, 1999.

27 Uyeda, S., Nagao, T., Kamogawa, M.: Short-term EQ prediction: Current status of seismo-  
28 electromagnetics, Tectonophysics, 470, 205–213, 2009a.

29 Uyeda, S., Kamogawa, M., Tanaka, H.: Analysis of electrical activity and seismicity in the  
30 natural time domain for the volcanic-seismic swarm activity in 2000 in the Izu Island  
31 region, Japan, J. Geophys Res., 114(B2), B02310, doi:10.1029/2007JB005332, 2009b.

32 Valkaniotis, S., Ganas, A., Papathanassiou, G., Papanikolau, M.: Field observations of  
33 geological effects triggered by the January-February 2014 Cephalonia (Ionian Sea,  
34 Greece) earthquakes, Tectonophysics, 630, 150-157, doi: 10.1016/j.tecto.2014.05.012,  
35 2014.

36 Vallianatos, F., Michas, G., Hloupis, G.: Multiresolution wavelets and natural time analysis  
37 before the January-February 2014 Cephalonia (Mw6.1 & 6.0) sequence of strong  
38 earthquake events, Phys. Chem. Earth, 85-86, 201–209, 2015.

39 Vamvakaris, D. A., Papazachos, C. B., Papaioannou, Ch. A., Scordilis, E. M., and Karakaisis,  
40 G. F.: A detailed seismic zonation model for shallow earthquakes in the broader Aegean  
41 area, Nat. Hazards Earth Syst. Sci., 16, 55-84, doi:10.5194/nhess-16-55-2016, 2016.

1 Varotsos, P. A.: *The Physics of Seismic Electric Signals*, TERRAPUB, Tokyo, 2005.

2 Varotsos, P. A., Sarlis, N. V., Skordas, E. S.: Spatio-temporal complexity aspects on the  
3 interrelation between seismic electric signals and seismicity., Pract. Athens Acad., 76,  
4 294-321, 2001.

5 Varotsos, P. A., Sarlis, N. V., Skordas, E. S.: Long-range correlations in the electric signals  
6 that precede rupture, Phys. Rev. E, 66, 011902.doi:10.1103/ PhysRevE.66.011902,  
7 2002.

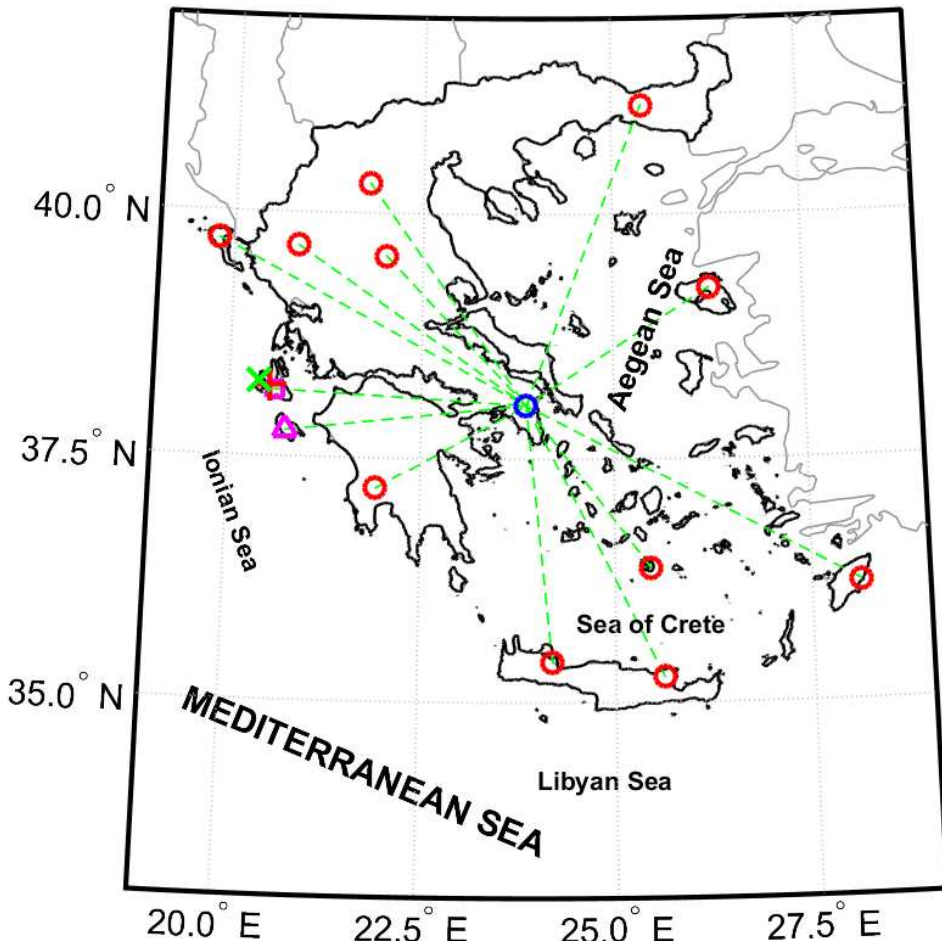
8 Varotsos, P. A., Sarlis, N. V., Tanaka, H. K., Skordas, E. S.: Similarity of fluctuations in  
9 correlated systems: The case of seismicity, Phys. Rev. E, 72, 041103. doi:  
10 10.1103/PhysRevE.72.041103, 2005.

11 Varotsos, P. A., Sarlis, N. V., Skordas, E. S., Tanaka, H. K., Lazaridou, M. S.: Entropy of  
12 seismic electric signals: Analysis in the natural time under time reversal, Phys. Rev. E,  
13 73, 031114. doi:10.1103/PhysRevE.73.031114, 2006.

14 Varotsos, P., Sarlis, N., Skordas, E., Uyeda, S., Kamogawa, M.: Natural time analysis of  
15 critical phenomena, Proc. Natl. Acad. Sci. USA, 108, 11361–11364, 2011a.

16 Varotsos, P., Sarlis, N., Skordas, E. S.: *Natural Time Analysis: The New View of Time*,  
17 Springer, Berlin, 2011b.

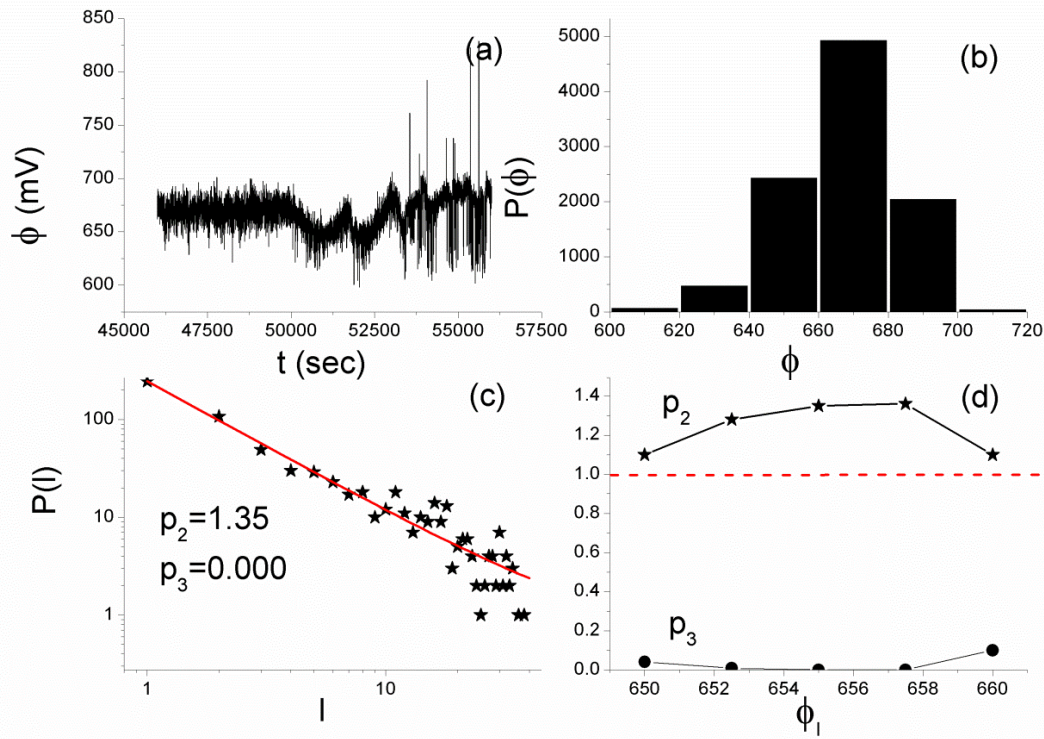
18 Wanliss, J., Muñoz, V., Pastén, D., Toledo, B., Valdivia, J. A.: Critical behavior in earthquake  
19 energy dissipation, Nonlin. Processes Geophys. Discuss., 2, 619–645, 2015.

1  
2  
3**Figures**

4  
5 **Figure 1.** Map with distribution of stations of the telemetric network that monitors  
6 electromagnetic variations in the MHz and kHz bands in Greece, which were operating during  
7 the time period of interest. The locations of the Cephalonia and Zante stations are marked by  
8 the magenta square and triangle, respectively, while the rest of the remote stations are denoted  
9 by red circles and the central data recording server by a blue circle. The epicenters of the two  
10 significant EQs of interest are also marked, the first (EQ1,  $M_w = 6.0$ ) by a red cross and the  
11 second (EQ2,  $M_w = 5.9$ ) by a green X mark. The electromagnetic variations monitored at  
12 Zante station are 3 kHz North-South, 3 kHz East-West, 3 kHz Vertical, 10 kHz North-South,

1 10 kHz East-West, 10 kHz Vertical, 41 MHz, 54 MHz and 135 MHz, while at the rest of the  
 2 stations, including Cephalonia station, only the 3kHz North-South, 3kHz East-West, 10kHz  
 3 North-South, 10kHz East-West, 41MHz and 46MHz are recorded. More details on the  
 4 instrumentation of the telemetric network can be found in the supplementary downloadable  
 5 material of (Potirakis et al., 2015). (For interpretation of the references to colors, the reader is  
 6 referred to the online version of this paper.)

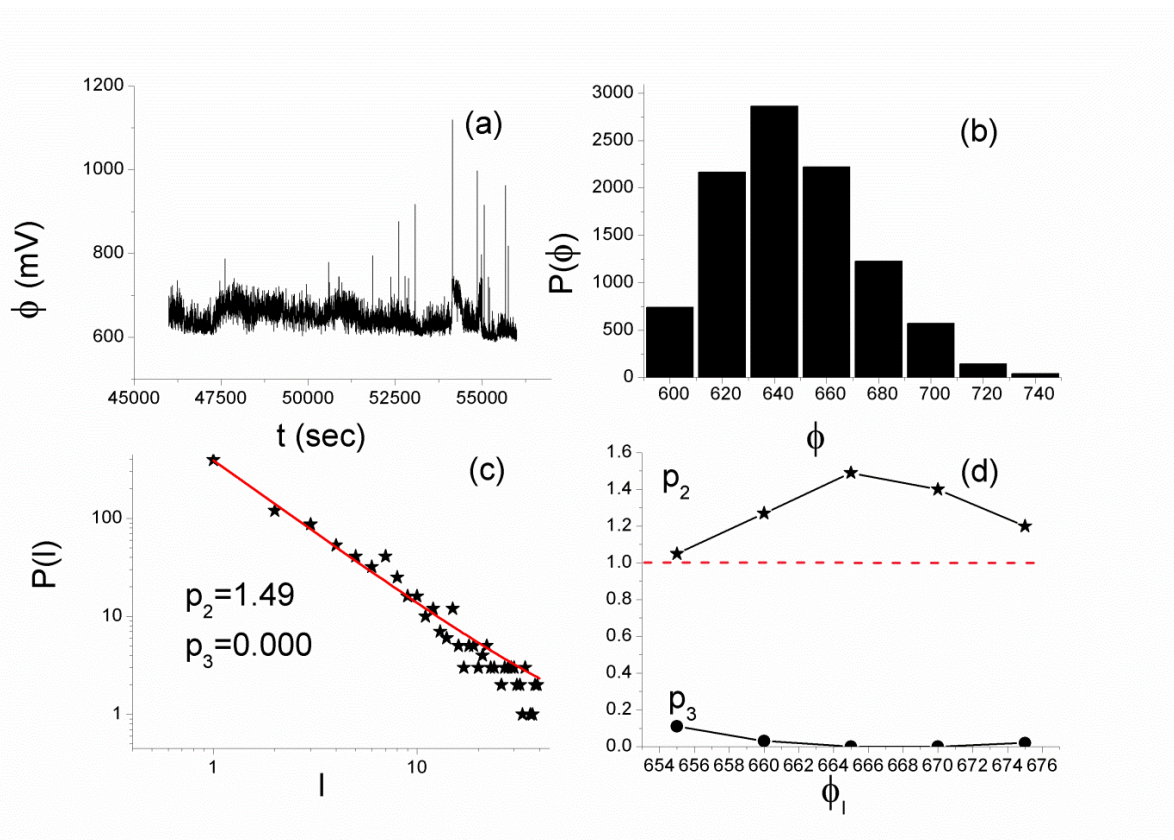
7



8

9 **Figure 2.** (a) The 10,000 samples long critical window of the MHz EME that was recorded  
 10 before the Cephalonia  $M_w = 6.0$  EQ at the Cephalonia station. (b) Amplitude distribution of  
 11 the signal of Fig. 2a. (c) Distribution of laminar lengths for the end point  $\phi_l = 655\text{mV}$ , as a  
 12 representative example of the involved fitting. The solid line corresponds to the fitted function  
 13 (cf. to text in Sec. 2.1) with the values of the corresponding exponents  $p_2$ ,  $p_3$  also noted. (d)  
 14 The obtained exponents  $p_2$ ,  $p_3$  vs. different values of the end of laminar region  $\phi_l$ . The  
 15 horizontal dashed line indicates the critical limit ( $p_2 = 1$ ).

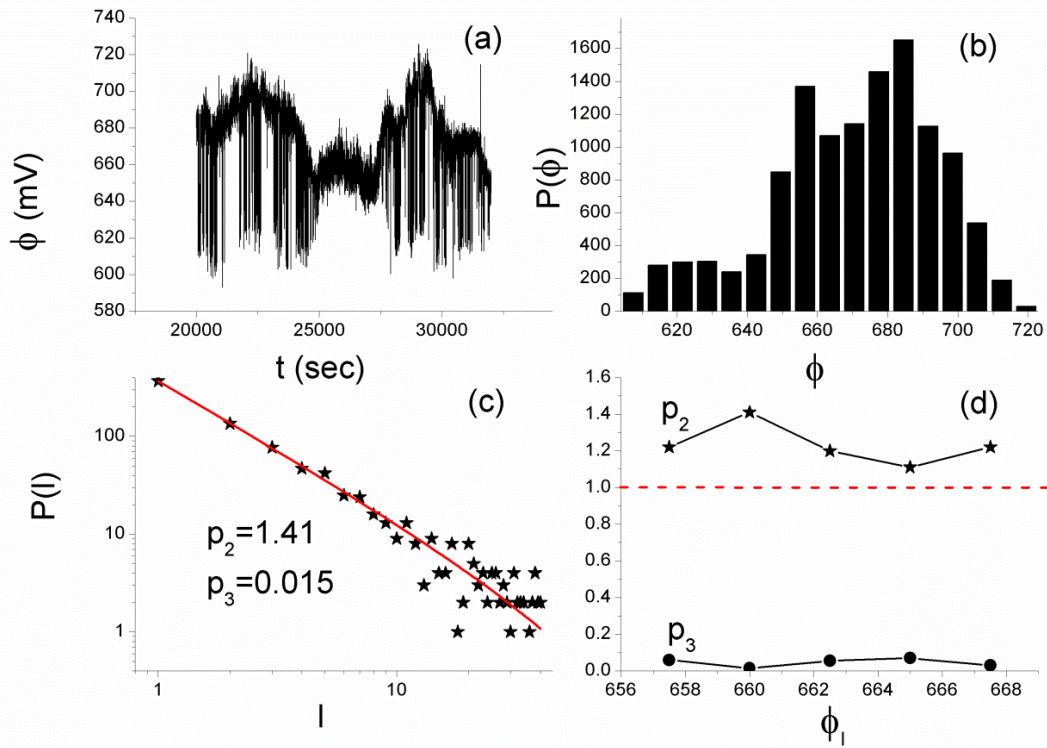
1



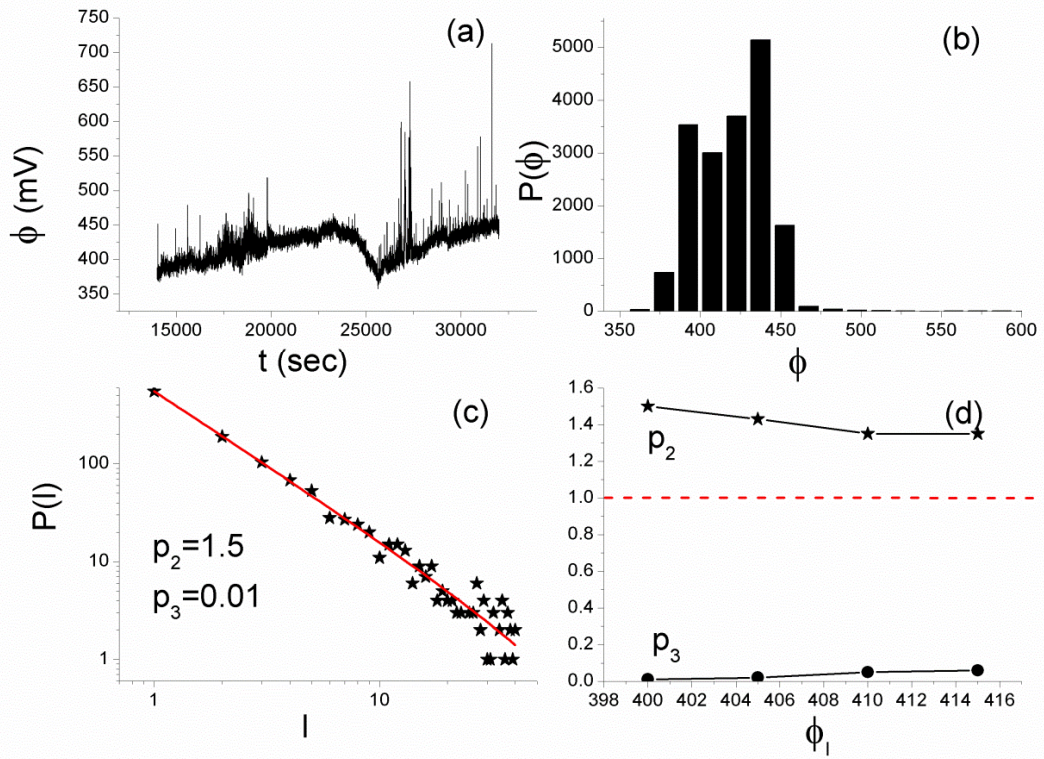
2

3 **Figure 3.** (a) The 10,000 samples long critical window of the MHz EME that was recorded  
 4 prior to the Cephalonia  $M_w = 6.0$  EQ at the Zante station, while (b), (c), and (d) are similar to  
 5 the corresponding parts of Fig. 2. From 3b, a fixed-point (start of laminar regions),  $\phi_o$  of  
 6 about 600 mV results, while in Fig. 3c, the distribution of laminar lengths is given for the end  
 7 point  $\phi_l = 665 mV$  for which the exponents  $p_2 = 1.49$ ,  $p_3 = 0.000$  with  $R^2 = 0.999$  were  
 8 obtained.

9



1  
2 **Figure 4.** (a) The 12,000 samples long critical window of the MHz EME that was recorded  
3 before the Cephalonia  $M_w = 5.9$  EQ at the Cephalonia station, while (b), (c), and (d) are  
4 similar to the corresponding parts of Fig. 2. In Fig. 4c, the distribution of laminar lengths is  
5 given for the end point  $\phi_l = 660$  mV .  
6



1  
2 **Figure 5.** (a) The 18,000 samples long critical window of the MHz EME that was recorded  
3 before the Cephalonia  $M_w = 5.9$  EQ at the Zante station; (b), (c), and (d) are similar to the  
4 corresponding parts of Fig. 2. In Fig. 5c, the distribution of laminar lengths corresponds to the  
5 end point  $\phi_l = 400mV$ .

6

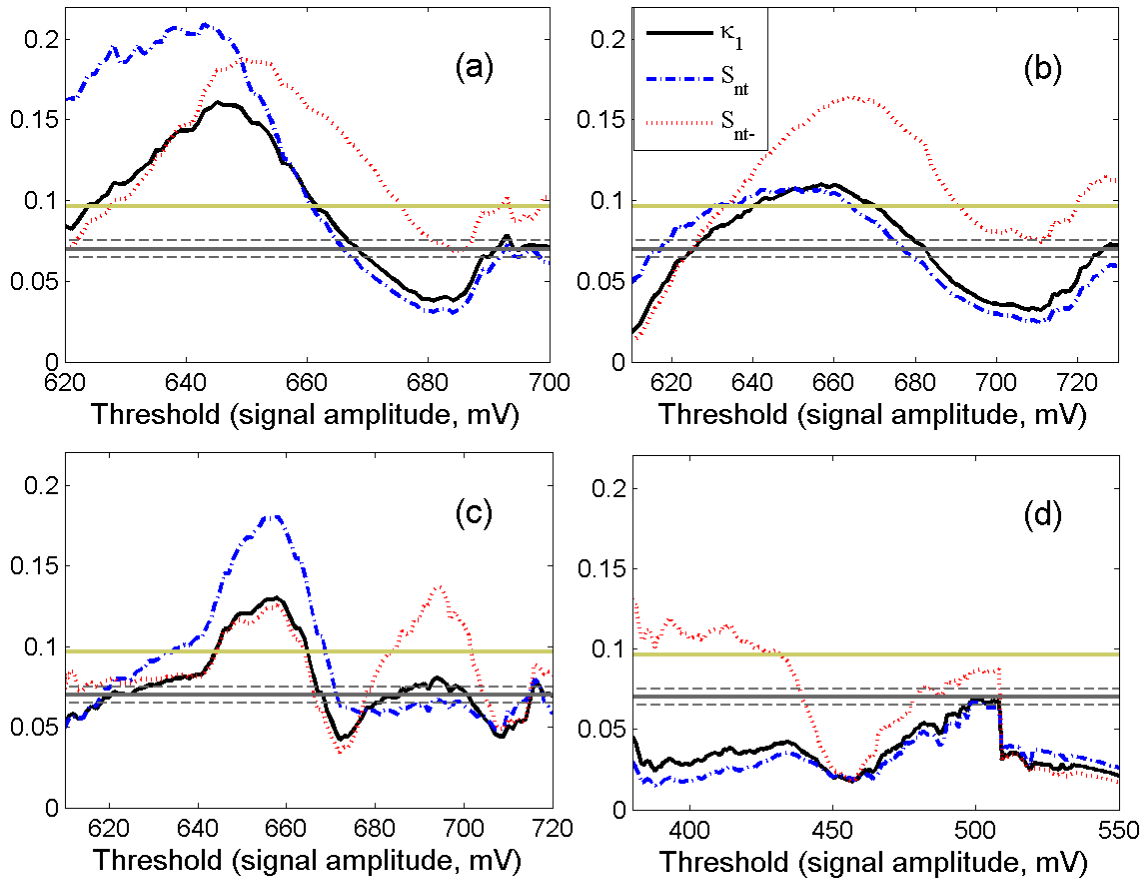
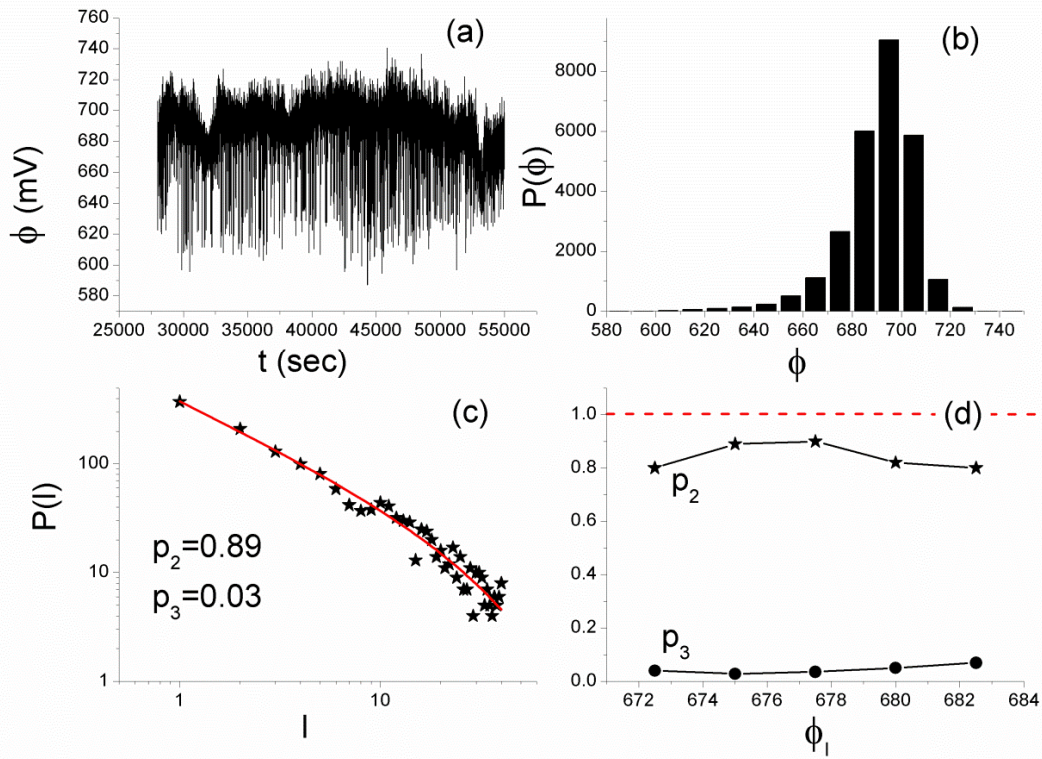
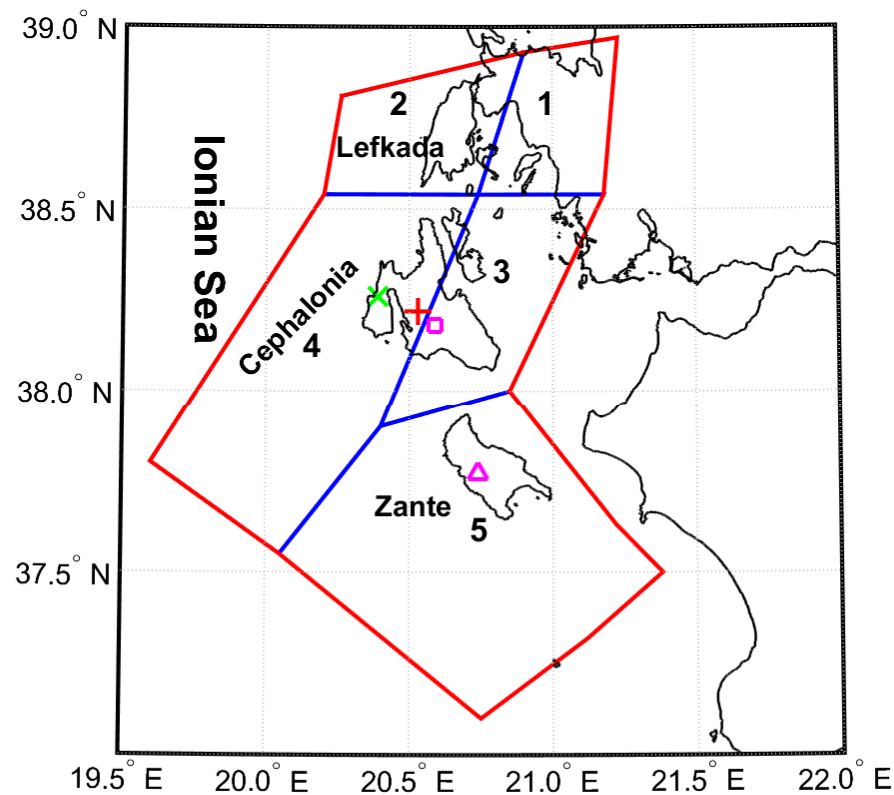


**Figure 6.** Natural time analysis results obtained for the MHz EME signals shown in: (a) Fig. 2a, recorded at Cephalonia station prior to EQ1, (b) Fig. 3a, recorded at Zante station prior to EQ1, (c) Fig. 4a, recorded at Cephalonia station prior to EQ2, and (d) Fig. 5a, recorded at Zante station prior to EQ2. The quantities  $\kappa_1$  (solid curve),  $S_{nt}$  (dash-dot curve), and  $S_{nt-}$  (dot curve) vs. amplitude threshold for each MHz signal are shown. The entropy limit of  $S_u$  ( $\approx 0.0966$ ), the value 0.070 and a region of  $\pm 0.005$  around it are denoted by the horizontal solid light green, solid grey and the grey dashed lines, respectively. (For interpretation of the references to colors, the reader is referred to the online version of this paper.)



1  
2 **Figure 7.** (a) The 27,000 samples long tricritical excerpt of the MHz EME that was recorded  
3 before the Cephalonia  $M_w = 5.9$  EQ at the Cephalonia station; (b), (c), and (d) are similar to  
4 the corresponding parts of Fig. 2. In Fig. 7c, the distribution of laminar lengths corresponds to  
5 the end point  $\phi_l = 675\text{mV}$ .

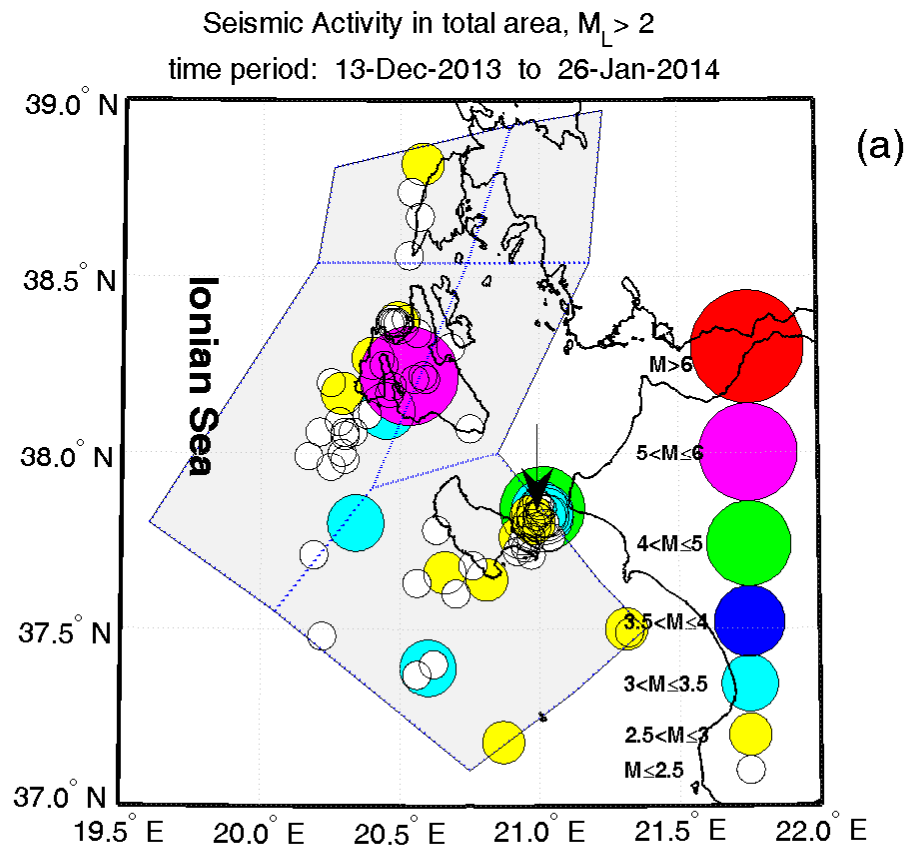
6

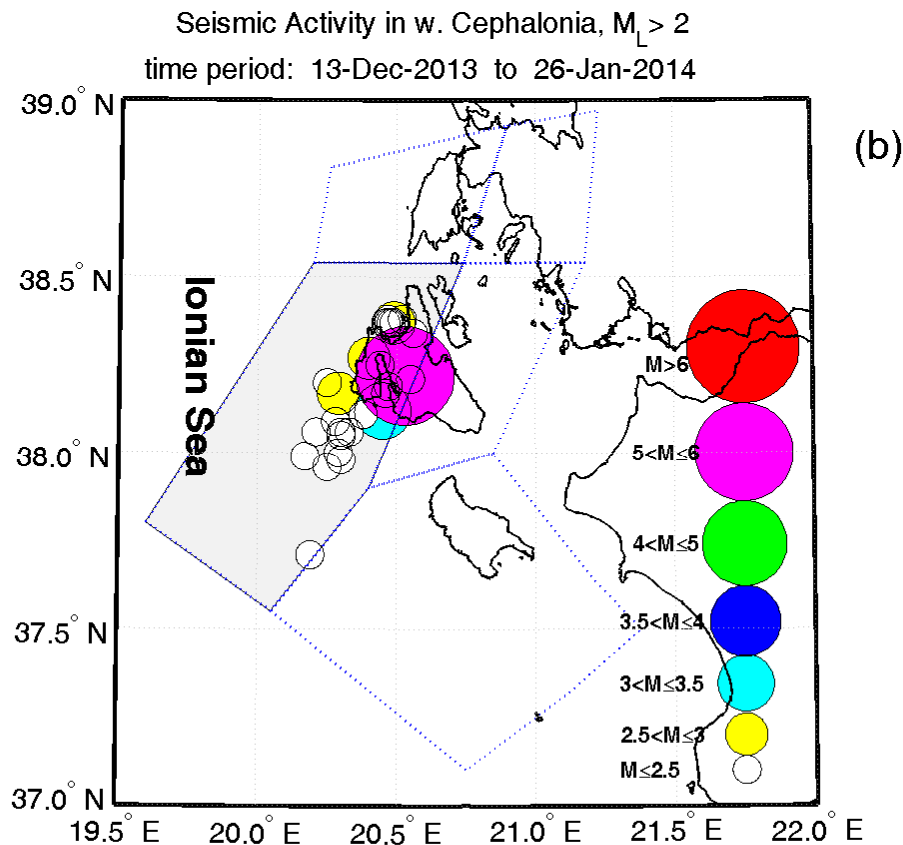


1

2 **Figure 8.** Seismic zonation in the Ionian Islands area. The locations of the Cephalonia and  
3 Zante stations, as well as the epicenters of the two significant EQs of interest are marked,  
4 using the same signs presented in Fig. 1.

5





1  
2 **Figure 9.** Foreshock seismic activity ( $M_L$ ) before EQ1: (a) for the whole investigated area of  
3 the Ionian Sea region; (b) for west Cephalonia. (For interpretation of the references to colors,  
4 the reader is referred to the online version of this paper.)  
5

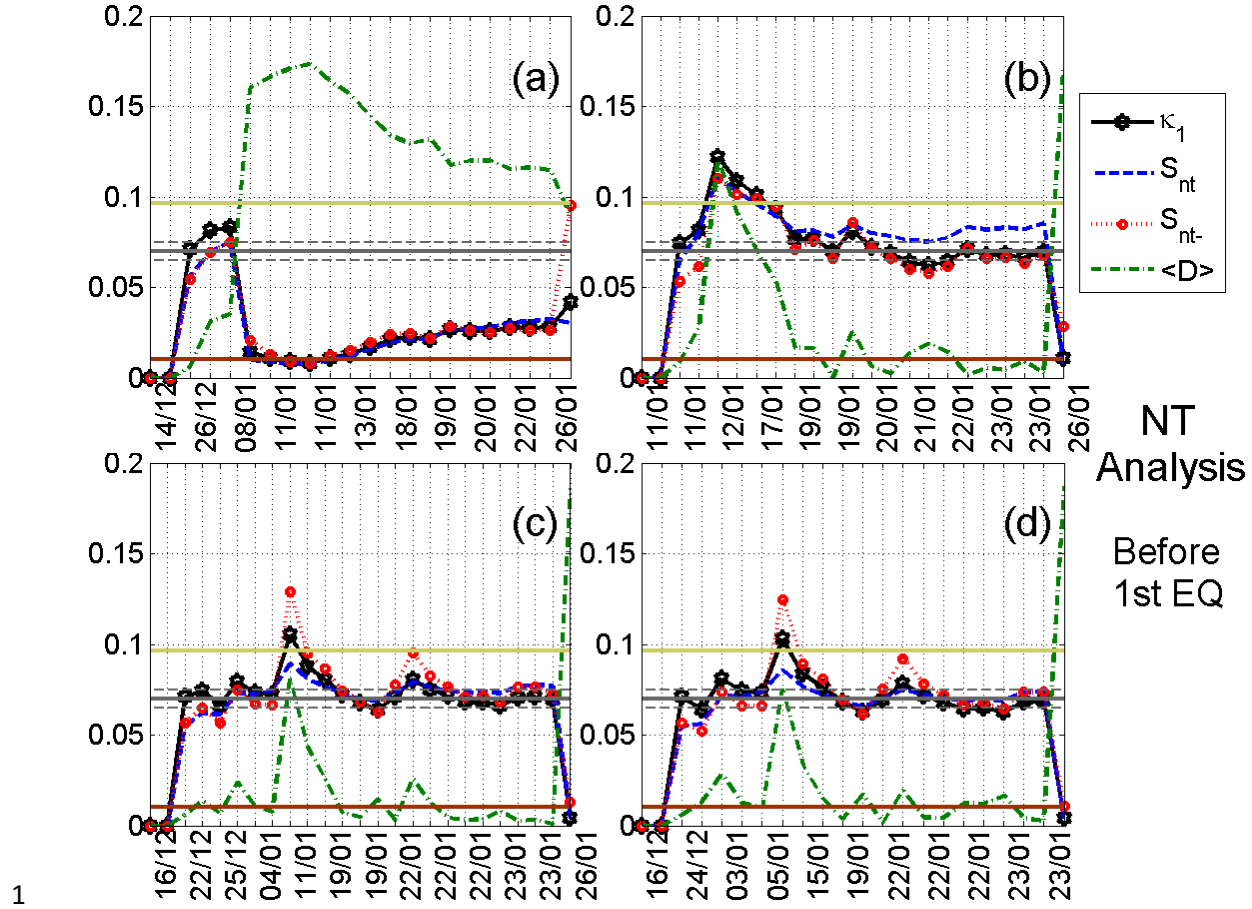
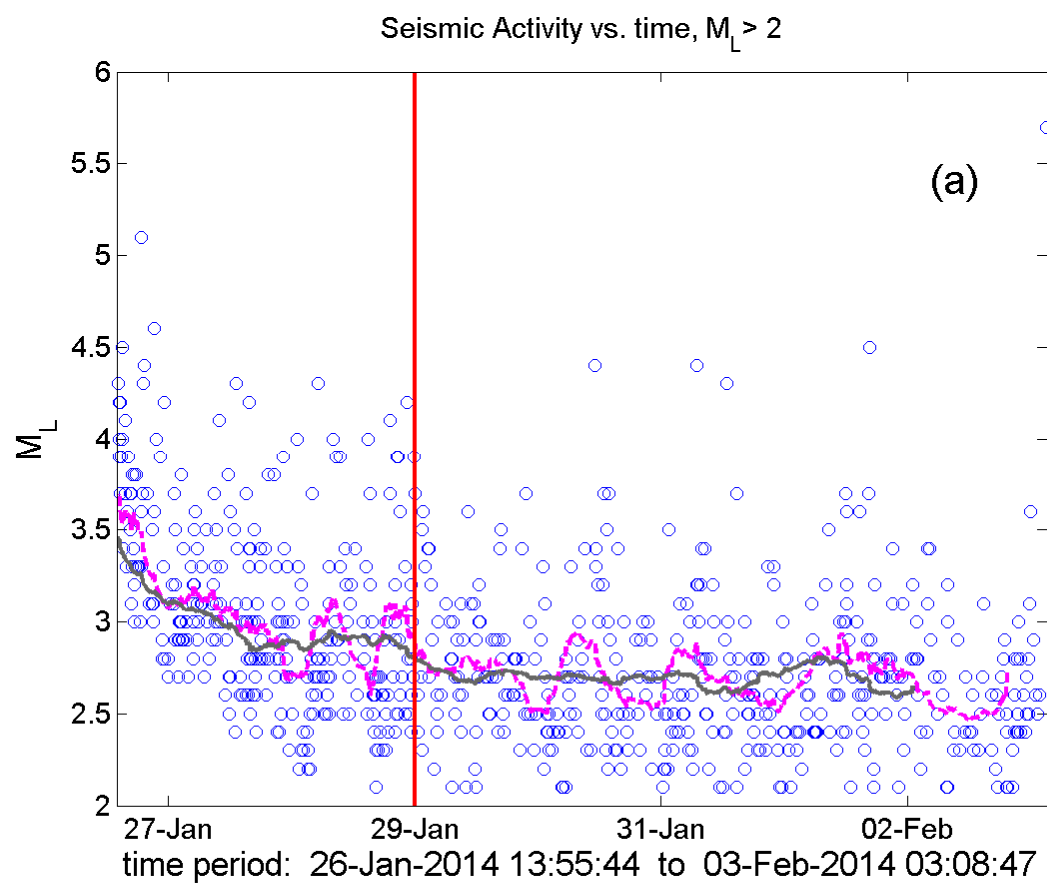
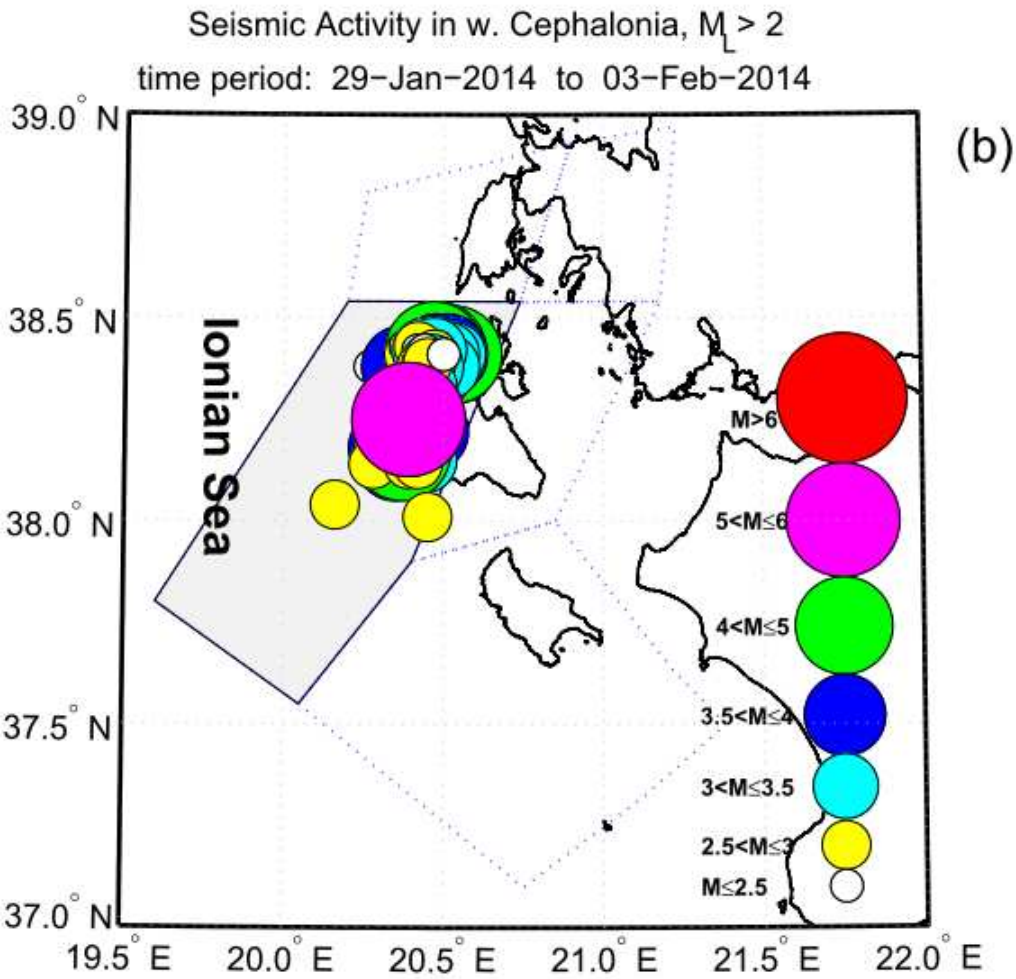


Figure 10. Temporal evolutions of the four natural time (NT) analysis parameters ( $\kappa_1$ ,  $S_{nt}$ ,  $S_{nt-}$ , and  $\langle D \rangle$ ) for the foreshock seismic activity recorded prior to EQ1: (a) for the activity of the whole investigated area of the Ionian Sea for  $M_L$  threshold 2.5, during the period from 13/12/2013 00:00:00 to 26/01/2014 13:55:44 UT (just after the occurrence of EQ1); (b) for the activity of the whole investigated area of the Ionian Sea for  $M_L$  threshold 2.3, during the period from 11/01/2014 04:13:00 (just after the  $M_L = 4.7$  occurred in Zante) to 26/01/2014 13:55:44 UT; (c) for the activity of both Cephalonia (east and west) zones combined for  $M_L$  threshold 2.1, during the period from 13/12/2013 00:00:00 to 26/01/2014 13:55:44 UT; (d) for the activity of the west Cephalonia for  $M_L$  threshold 2.1, during the period from 13/12/2013 00:00:00 to 26/01/2014 13:55:44 UT. Note that the events employed depend on the considered threshold. Moreover, the time (x-) axis is not linear in terms of the conventional date of occurrence of the events, since the employed events appear equally spaced relative to x-axis, as the natural time representation demands, although they are not

1 equally spaced in conventional time. The horizontal solid light green, solid grey and the grey  
2 dashed lines, denote the same quantities as in Fig. 6, while the horizontal solid brown line  
3 denotes the  $10^{-2}$  limit for  $\langle D \rangle$ . (For interpretation of the references to colors, the reader is  
4 referred to the online version of this paper.)

1  
2

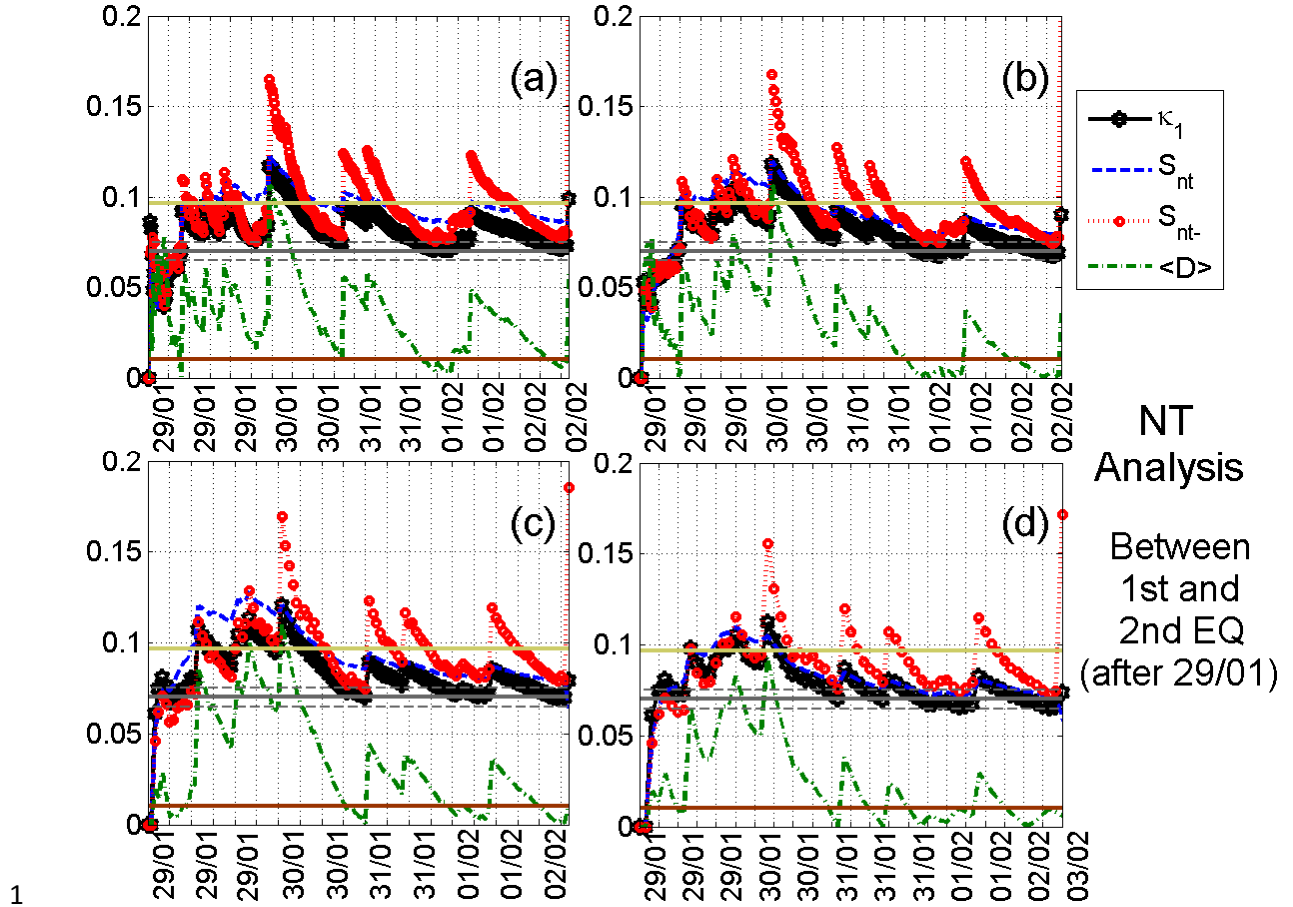
3



1 **Figure 11.** (a) Seismic activity from the time immediately after EQ1 ( $M_w = 6.0$ ) up to the  
2 time of EQ2 ( $M_w = 5.9$ ) for the whole investigated area of the Ionian Sea. The moving  
3 averages of the recorded earthquake local magnitudes vs. time for calculation windows of 25  
4 and 75 successive events are shown by the dashed magenta and solid grey curve, respectively.  
5 The vertical solid red line denotes the time point 29 January 00:00:00 UT. (b) The considered  
6 as foreshock seismic activity before EQ2 (from 29/01/2014 00:00 UT up to the time of  
7 occurrence of EQ2) for west Cephalonia. All presented magnitudes are local magnitudes  
8 ( $M_L$ ). (For interpretation of the references to colors, the reader is referred to the online  
9 version of this paper.)

10

11



1 **Figure 12.** Natural time (NT) analysis results for the seismicity in the partition of west  
2 Cephalonia during the time period from 29/01/2014 00:00:00 to 03/02/2014 03:08:47 UT  
3 (between EQ1,  $M_w = 6.0$ , and EQ2,  $M_w = 5.9$ ): (a)-(d) Temporal evolutions of the four  
4 natural time analysis parameters ( $\kappa_1$ ,  $S_m$ ,  $S_{m-}$ , and  $\langle D \rangle$ ) for the different  $M_L$  thresholds 2.2,  
5 2.6, 2.8, and 3.0, respectively. Note that the events employed depend on the considered  
6 threshold. Moreover, the time (x-) axis is not linear in terms of the conventional date of  
7 occurrence of the events, since the employed events appear equally spaced relative to x-axis,  
8 as the natural time representation demands, although they are not equally spaced in  
9 conventional time. The horizontal solid light green, solid grey and the grey dashed lines,  
10 denote the same quantities as in Fig. 6, while the horizontal solid brown line denotes the  $10^{-2}$   
11 limit for  $\langle D \rangle$ . (For interpretation of the references to colors, the reader is referred to the  
12 online version of this paper.)